Radiocarbon calibration curve spanning 0 to 50,000 years BP based on paired ^{230}Th/ ^{234}U/ ^{238}U and ^{14}C dates on pristine corals

Richard G. Fairbanks[a,b,*], Richard A. Mortlock[a], Tzu-Chien Chiu[a,b], Li Cao[a,b], Alexey Kaplan[a], Thomas P. Guilderson[c,d], Todd W. Fairbanks[e], Arthur L. Bloom[f], Pieter M. Grootes[g], Marie-Josée Nadeau[g]

[a]*Lamont Doherty Earth Observatory, Columbia University, Rt. 9W, Palisades, NY 10964, USA*
[b]*Department of Earth & Environmental Sciences, Columbia University, Rt. 9W, Palisades, NY 10964, USA*
[c]*Center for Accelerator Mass Spectrometry, Lawrence Livermore National Laboratory, Livermore, CA 94551, USA*
[d]*Department of Ocean Sciences, University of California – Santa Cruz, 1156 High Street, Santa Cruz, CA 94056, USA*
[e]*Columbia University, 1864 Lerner Hall, New York, NY 10027-8311, USA*
[f]*Department of Earth and Atmospheric Sciences, Cornell University, 2122 Snee Hall, Ithaca, NY 14853-1504, USA*
[g]*Leibniz Laboratory for Radiometric Age Determination and Isotope Research, Christian Albrecht University, 24118 Kiel, Germany*

Abstract

Radiocarbon dating is the most widely used dating technique in the world. Recent advances in Accelerator Mass Spectrometry (AMS) and sample preparation techniques have reduced the sample-size requirements by a factor of 1000 and decreased the measurement time from weeks to minutes. Today, it is estimated that more than 90 percent of all measurements made on accelerator mass spectrometers are for radiocarbon age dates. The production of ^{14}C in the atmosphere varies through time due to changes in the Earth's geomagnetic field intensity and in its concentration, which is regulated by the carbon cycle. As a result of these two variables, a radiocarbon age is not equivalent to a calendar age. Four decades of joint research by the dendrochronology and radiocarbon communities have produced a radiocarbon calibration data set of remarkable precision and accuracy extending from the present to approximately 12,000 calendar years before present. This paper presents high precision paired ^{230}Th/ ^{234}U/ ^{238}U and ^{14}C age determinations on pristine coral samples that enable us to extend the radiocarbon calibration curve from 12,000 to 50,000 years before present. We developed a statistical model to properly estimate sample age conversion from radiocarbon years to calendar years, taking full account of combined errors in input ages and calibration uncertainties. Our radiocarbon calibration program is publicly accessible at: http://www.radiocarbon.LDEO.columbia.edu/ along with full documentation of the samples, data, and our statistical calibration model.
© 2005 Elsevier Ltd. All rights reserved.

1. Introduction

The records of the ^{14}C content of the atmosphere and oceans contain a remarkable array of information about Earth history (Arnold and Libby, 1949; Libby, 1955; Suess, 1970; Damon et al., 1978; Stuiver, 1982; Stuiver and Pearson, 1986; Damon, 1988; Bard, 1998). Pro-duced by cosmic rays in the upper atmosphere (Lal and Peters, 1962; Suess 1968; Lal, 1988), ^{14}CO$_2$ rapidly mixes throughout the troposphere and exchanges with the reactive carbon reservoirs of the oceans and biosphere, where it decays (Suess, 1955; Craig, 1957; de Vries 1958, 1959). For the past 11,000 years, fluctuations in the atmospheric ^{14}C have been largely produced by changes in the solar magnetic field (de Vries, 1958, 1959; Stuiver, 1961; Stuiver and Quay, 1980). Most recently, Goslar et al. (2000a) concluded that variations in solar activity were the primary cause

*Corresponding author. Tel.: +1 845 365 8499.
E-mail address: fairbanks@LDEO.columbia.edu
(R.G. Fairbanks).

of the larger atmospheric ^{14}C fluctuations for the period 11,000 to 14,500 years before present, although many researchers believe that carbon cycle changes tied to deep ocean circulation are a significant cause of atmospheric ^{14}C fluctuations in this time interval (Edwards et al., 1993; Mikolajewicz, 1996; Stocker and Wright, 1996; Hughen et al., 2000; Muscheler et al., 2000; Delaygue et al., 2003). On longer time scales, changes in the Earth's magnetic field intensity impact the ^{14}C content of the atmosphere, producing positive ^{14}C anomalies during intervals of weaker geomagnetic field strength (Elsasser et al., 1956; McElhinny and Senanayake, 1982; Damon, 1988; Beer et al., 1988; Bard et al, 1990; Guyodo and Valet, 1999; Laj et al., 2000, 2004; Voelker et al., 2000). Of practical importance to a wide range of scientific disciplines is the radiocarbon calibration, which is used to convert radiocarbon ages to calendar years and to compute changes in atmospheric ^{14}C ($\Delta ^{14}$C) through time (Stuiver, 1982; Damon, 1988; Bard et al., 1990, 1993; Edwards et al., 1993; Stuiver et al., 1986, 1998a, b; Burr et al., 1998; Hughen et al., 2000; Goslar et al., 2000c; Schramm et al., 2000; Voelker et al., 2000; Beck et al., 2001). Accurate calibration of radiocarbon ages to calendar years is essential for measuring time and rates of change for numerous scientific fields. According to Kutschera (1999), nearly 90% of all measurements made at the more than 50 active accelerator mass spectrometry laboratories are radiocarbon analyses.

The widely accepted tree ring radiocarbon calibration data set and resulting calibration curve are based on radiocarbon measurements of wood that has been absolutely dated by counting annual growth rings in overlapping tree chronologies (Stuiver, 1982; Damon, 1988; Stuiver et al., 1998a, b; Reimer et al., 2004). The continuous tree ring radiocarbon calibration spans from the present to nearly 12,000 yr BP. Suitable trees older than 12,000 yr BP are rare, but efforts continue to extend the tree ring calibration curve (Friedrich et al., 1999, 2001, 2004). In this study, we have overlapped and extended the tree-ring radiocarbon calibration from 0 to 50,000 yr BP using coral samples from our offshore coral reef core collection from Barbados (13.10°N; 59.32°W) in the western tropical Atlantic and Kiritimati Atoll (1.99°N, 157.78°W) in the central equatorial Pacific, and from the uplifted reefs of Araki Island (15.63°S; 166.93°E) in the western Pacific (Chiu et al., 2004, 2005a). Using new pretreatment and analytical techniques and state-of-the-art instrumentation at higher precision, we have reanalyzed the radiocarbon and ^{230}Th/^{234}U/^{238}U age dates from our original calibration work (Fairbanks, 1989, 1990; Bard et al., 1990, 1993, 1998), all of which were included in INTCAL98 (Stuiver et al., 1998a). These new results are reported in Appendix A.

In this paper, we present paired ^{230}Th/^{234}U/^{238}U (Lamont) and ^{14}C age determinations (Lawrence Livermore National Lab and Leibniz-Labor for Radiometric Dating and Isotope Research Christian-Albrechts University Kiel) that span the entire range of the radiocarbon dating technique and present a radiocarbon calibration curve based on a Bayesian statistical model with rigorous error estimations. Our radiocarbon calibration curve is a stand-alone alternative to existing radiocarbon calibration data sets that infer calendar ages based on interpolations and correlations of local climate proxies in deep sea cores to the chronology of ice core proxies or assumptions about sedimentation rates (Voelker et al., 2000; Kitagawa and van der Plicht, 2000; Hughen et al., 2004a). Our calibration meets the requirements that each data point in the calibration has a measured calendar age (^{230}Th/^{234}U/^{238}U) and radiocarbon age with known errors that are independent of each other. We have chosen not to include coral data from other studies (Yokoyama et al., 2000; Paterne et al., 2004; Cutler et al., 2004; Hughen et al., 2004b) because coral samples reported in the literature typically contain between 1% and 5% calcite, a contaminant which is significantly concentrated during the sample-etching step prior to radiocarbon analyses, thereby corrupting the radiocarbon data (Chiu et al., 2005). In addition, we choose not to include coral samples that reported calcite detection limits above 0.2% (Bard et al., 1998), even if no calcite was reported in a sample, because samples contaminated by more than 0.2% are generally unsuitable for calibration purposes (Chiu et al., 2005), particularly for older samples. Finally, we have reanalyzed all of our previous radiocarbon calibration measurements on our Barbados samples (Fairbanks 1989, 1990; Bard et al., 1990, 1993, 1998; Stuiver et al., 1998a, b) at higher precision and with many replicates for both radiocarbon and ^{230}Th/^{234}U/^{238}U, so we have not included these earlier measurements in our calibration curve. In the following sections, we outline our sample selection criteria, pretreatment procedures, analytical methods, Bayesian statistical model, and present our calibration curve.

2. Radiocarbon age calibration

2.1. Paired ^{230}Th/^{234}U/^{238}U and ^{14}C age dating of corals

Radiocarbon ages must be converted to calendar ages via an independent chronometer for accurate dating applications. Radiocarbon ages spanning the last 11,900 years are calibrated by making radiocarbon age determinations on tree rings of known age (Damon and Long, 1962; Damon et al., 1963; Stuiver et al.,

1998a, b; Spurk et al., 1998; Friedrich et al., 1999; Reimer et al., 2002, 2004). For the age interval between 12,000 years and 50,000 years before present, radiocarbon ages are calibrated by less precise and less accurate methods, such as varved sediments (Hughen et al., 1998, 2000, 2004b; Schramm et al., 2000; Goslar et al., 2000a, c; Kitagawa and van der Plicht, 2000; Hughen et al., 2004b; van der Plicht et al., 2004), correlation of distinct fluctuations in ocean/climate proxies dated by radiocarbon with similar features in the Greenland ice cores dated by layer counting and flow models (Hughen et al., 2000, 2004a; Voelker et al., 2000), ^{230}Th/ ^{234}U/ ^{238}U dating of speleothems (Vogel and Kronfeld, 1997; Goslar et al., 2000b; Beck et al., 2001) and corals (Fairbanks, 1990; Edwards et al., 1993; Bard et al., 1990, 1998a, b; Burr et al., 1998; Yokoyama et al., 2000; Cutler et al., 2004; Paterne et al., 2004; van der Plicht et al., 2004).

Each calibration approach has unique advantages and disadvantages. For example, it is possible that varved sediments can be dated precisely but not accurately due to missing or indistinct layers that lead to accumulating errors. Speleothems provide long records and are very useful for identifying general trends and maybe large ^{14}C production anomalies, but speleothems are potentially limited by the dating errors due to variable groundwater uranium-series and carbon chemistry. ^{230}Th/ ^{234}U/ ^{238}U dating of corals can be reasonably precise and accurate, but samples of appropriate age are hard to acquire and the coral ^{230}Th/ ^{234}U/ ^{238}U ages can be altered by freshwater diagenesis (Hamelin et al., 1991; Henderson et al., 1993; Gallup et al., 1994, 2002; Ribaud-Laurenti et al., 2001), and in some locations by marine cements (Ribaud-Laurenti et al., 2001; Paterne et al., 2004). Even trace amounts of diagenetic calcite deposited in subaerially exposed corals will bias the radiocarbon measurements (Chiu et al., 2005a). In addition, ancient coral samples must be used for radiocarbon blanks because biogenic carbonate blanks are generally higher than spar calcite typically used in AMS laboratories. Attempts to develop a radiocarbon calibration curve by making radiocarbon measurements of microfossils in cores that contain proxies that can be correlated to ice core proxies have compounded errors due to proxy interpretations, correlation errors, and large uncertainties in ice-core chronologies (Hughen et al., 2000, 2004a; Voelker et al., 2000). Over the radiocarbon calibration interval, there are generally fewer than thirty tie points correlating deep sea core ocean/climate proxies to ice core proxies, thereby assigning calendar age estimates to most calibration points by interpolation. Differences between the various Greenland ice core chronologies are due to age model assumptions, inherent subjectivity in discerning annual bands in ice or layered sediments in general, the fidelity of proxies to record an annual signal, occasional wind

erosion or scouring of some snow layers, and compacting and degrading annual signals deeper in the ice cores (Dansgaard et al., 1989, 1993; Johnsen et al., 1992, 1995, 1997, 2001; Meese et al., 1994, 1997; Taylor et al., 1993; Stuiver et al., 1995; Andersen et al., 2004). Intervals where the annual signal is weak or missing entirely would not be counted by any of the proxies and therefore not included in Meese et al.'s (1997) error assessment. Another reason to avoid calibrating the radiocarbon timescale to ice core chronologies is the fact that many paleoclimate studies reference marine or terrestrial proxies to the ice core records of atmospheric gas chemistry, and these chronologies must remain independent for reliable interpretations.

All radiocarbon ages are readily subject to contamination by modern carbon during sample handling and processing of samples. In many cases, the different calibration archives are complementary and atmosphere and ocean calibration data sets from different locations and different archives are necessary to improve the accuracy and precision of ongoing international calibration efforts such as INTCAL98 (Stuiver et al., 1998a) and newer calibration data sets (e.g. IntCal04, Reimer et al., 2002, 2004; Marine04, Hughen et al., 2004b).

Unfortunately, combining published radiocarbon calibration data greater than 12,000 yr BP results in a confusing and inaccurate calibration data set (Fig. 1). Offsets and contradictions are the norm among these various calibration data sets, in stark contrast with the remarkably high quality tree ring calibration set for the present to 11,900 yr BP. Our contributions to the international radiocarbon calibration effort are the ^{230}Th/ ^{234}U/ ^{238}U and ^{14}C analyses of a suite of unusually high quality coral samples. Importantly, overlapping tropical Atlantic and Pacific calibration data sets are particularly helpful in constraining the uncertainties in the ^{14}C reservoir age and validating fine details in those instances where the signals are coherent between oceans. It is our goal to construct a complete calibration data set using only pure aragonite coral samples, applying our rigorous pretreatment procedures outlined below, and measured with high precision mass spectrometry for ^{230}Th/ ^{234}U/ ^{238}U and ^{14}C measurements with abundant replicate analyses.

Another important reason to develop a stand alone coral calibration curve is the fact that ^{230}Th/ ^{234}U/ ^{238}U and ^{14}C ages have independent errors that can be measured and therefore, we can compute a rigorous error estimate for our radiocarbon calibration curve and calibrated radiocarbon ages. In contrast, radiocarbon calibration curves developed from floating varved sequences do not permit a rigorous error estimate of the calendar year due to the potential for an accumulation of errors in these sequences and inherent uncertainties in the age models. In addition, the accuracy and precision of our calibration data set can be tested by:
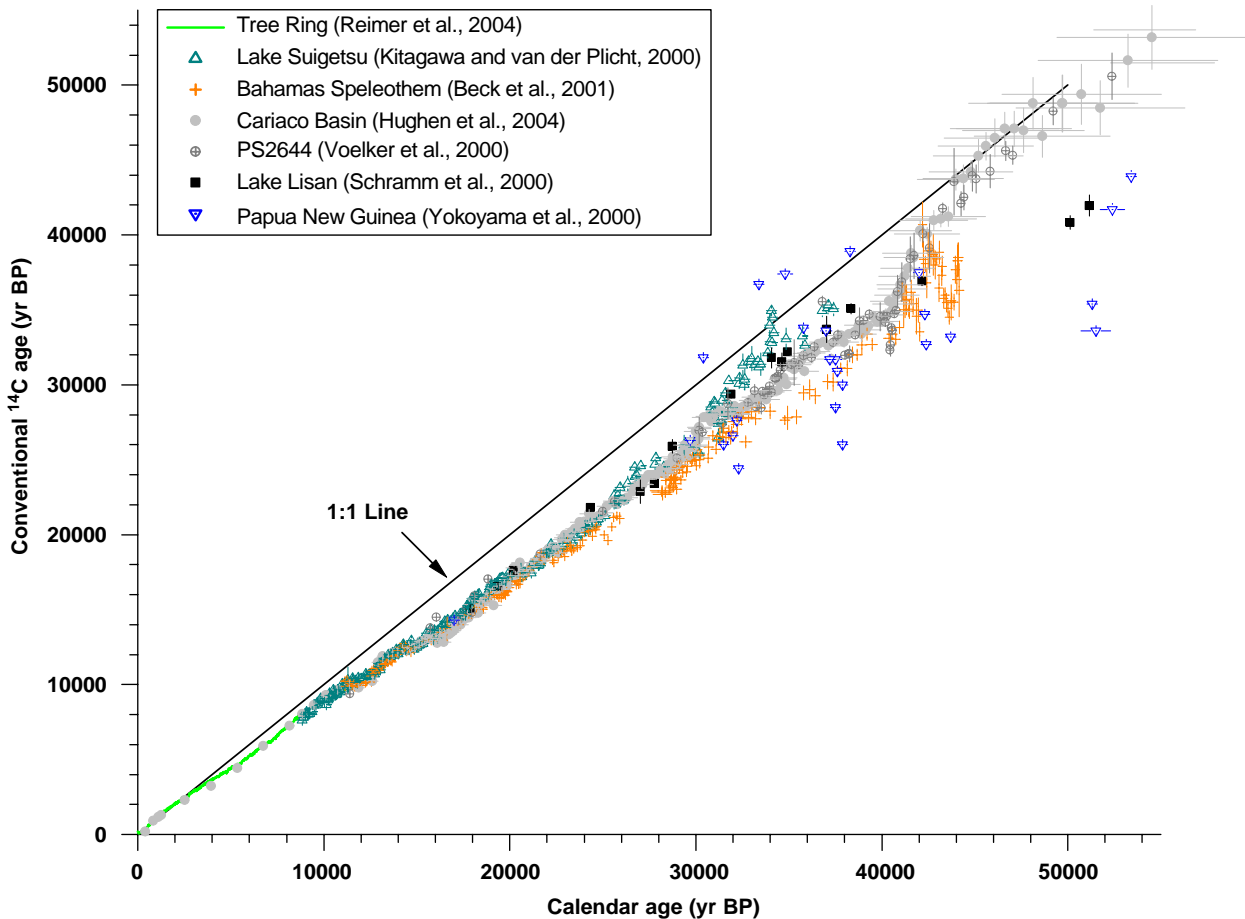
Fig. 1. Composite figure showing the range of radiocarbon calibration data from a variety of archives, including Bahamian speleothems (Beck et al., 2001), marine sediments (Hughen et al., 2000, 2004a; Voelker et al., 2000; lake sediments (Schramm et al., 2000; Kitagawa and van der Plicht, 2000), corals (Yokoyama, 2000), and tree rings (Reimer et al., 2004; Friedrich et al., 2004).

(a) measuring samples that overlap the tree ring calibration (Fig. 2); (b) making paired $^{230}Th/$ $^{234}U/$ ^{238}U and $^{231}Pa/$ ^{235}U ages on select samples (Pickett et al., 1994; Edwards et al., 1997; Cutler et al., 2004; Mortlock et al., 2005); and (c) through $^{230}Th/$ $^{234}U/$ ^{238}U, $^{231}Pa/$ ^{235}U and ^{14}C measurements of our inter-laboratory calibration samples that are a subset of our calibration data. These calibration samples range from the modern to 50,000 yr BP at 10,000-year increments and are distributed to interested laboratories.

The direct determination of ^{230}Th, ^{234}U, and ^{238}U abundances by Thermal Ionization Mass Spectrometry (TIMS) opened a wide range of dating applications that were previously out of reach of the classical alpha-counting technique (Chen et al., 1986; Edwards et al., 1987a, b; Edwards, 1988; Bard et al., 1990; Gallup et al., 2002). The typical 2σ precision of a mass spectrometry $^{230}Th/$ $^{234}U/$ ^{238}U date is better than 1% of the age (Chen et al., 1986; Edwards et al., 1987a, b; Mortlock et al., 2004). An early application of high precision $^{230}Th/$ $^{234}U/$ ^{238}U dating was paired $^{230}Th/$ $^{234}U/$ ^{238}U and ^{14}C age dating of coral samples, thereby extending

the radiocarbon calibration beyond that based on tree rings (Bard et al., 1990; Fairbanks, 1990; Edwards et al., 1993) to approximately 20,000 yr BP.

In addition to measuring new samples from Barbados, we have reanalyzed all of our original Barbados samples presented in Fairbanks (1989, 1990), Bard et al. (1990, 1993, 1998), and Stuiver et al. (1998a,b) at higher $^{230}Th/$ $^{234}U/$ ^{238}U precision using our Fisons Plasma 54, and paired these data with new higher precision ^{14}C analyses measured at the Lawrence Livermore National Lab (LLNL) Center for Accelerator Mass Spectrometry (CAMS) and Leibniz-Labor for Radiometric Dating and Isotope Research at Christian-Albrechts University Kiel. We have adopted the new half-life estimates for ^{230}Th and ^{234}U reported by Cheng et al. (2000) and report all data using these new values. Improvements to the sample pretreatment and quality control have been implemented (Chiu et al., 2005) and many of our new measurements include replicate analyses. In addition, we made 80 paired (including many replicates) $^{230}Th/$ $^{234}U/$ ^{238}U and ^{14}C measurements from our Kiritimati cores collected in an offshore wire-line
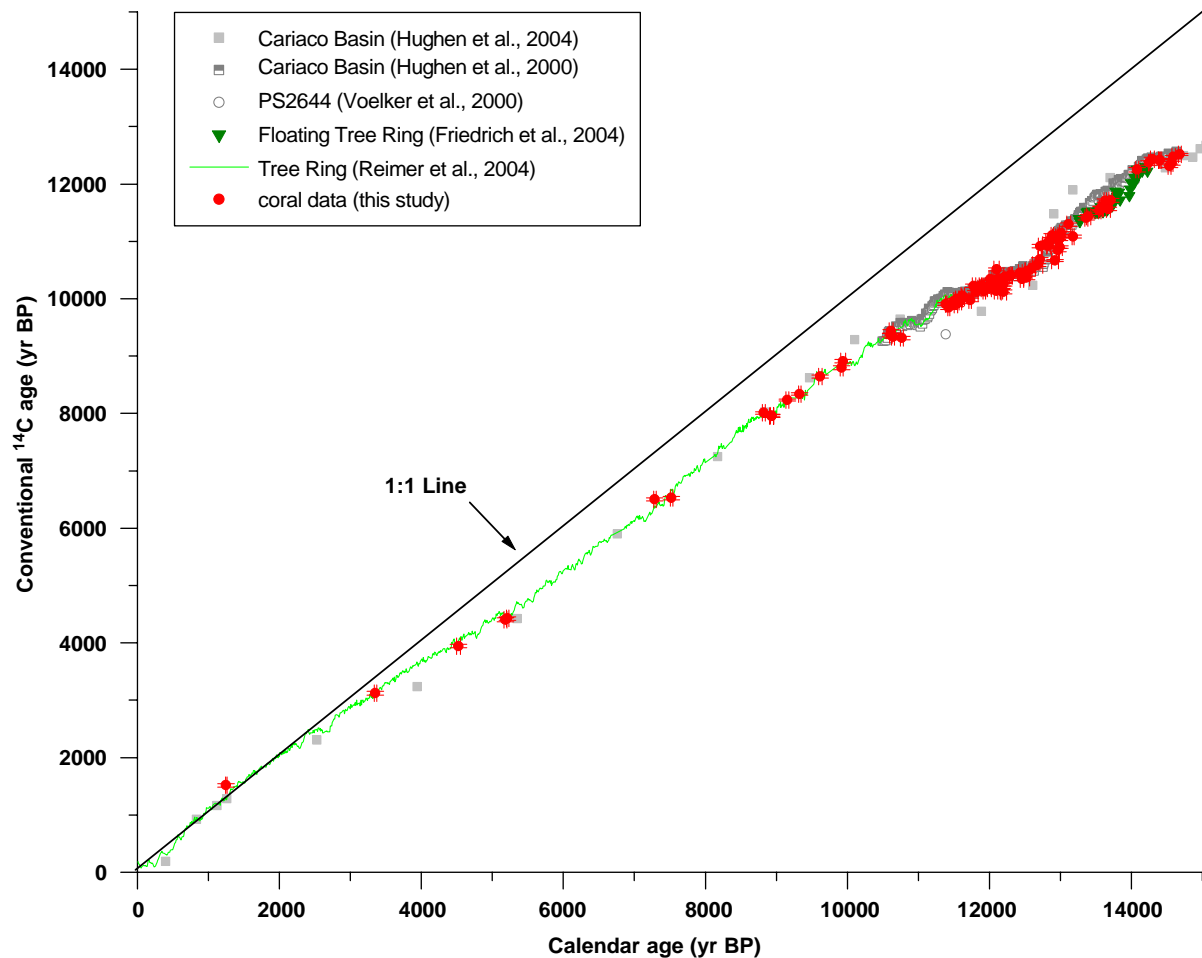
Fig. 2. Comparison of our coral data to the tree ring records of Reimer et al. (2004) and Friedrich et al. (2004) and the marine sediment data with calendar chronologies based on overlap with the tree ring data set and correlation to the oxygen isotope record in Greenland ice cores (Hughen et al., 2000, 2004a; Voelker et al., 2000). Note the consistency of our coral data with Friedrich et al.'s (2004) floating tree ring chronology, and where both diverge from the Cariaco (Hughen et al., 2000, 2004b) varved sequence between 13,300 and 14,000 yr BP. Figure zoom feature available at: http://www.radiocarbon.Ideo.Columbia.edu.

drilling program in 1998/99 from the central Pacific. Samples dated older than 34,000 yr BP are from the uplifted reefs of Araki Island (15.63°S; 166.93°E) located in the southwest Pacific. These new results are presented and discussed in this paper (Fig. 3). A subset of our paired dates younger than 26,000 yr BP are included in the IntCal04 calibration papers (Reimer et al., 2004; Hughen et al., 2004b).

During the next 3 years, we plan to make approximately 400 new $^{230}Th/ ^{234}U/ ^{238}U$ and ^{14}C measurements to fill in the gaps and details of the radiocarbon calibration from 0 to 50,000 yr BP. Our goal is to provide samples at approximately 100-year resolution or better. Our unique advantage is the quality of our coral samples from our offshore coring programs, combined with high precision $^{230}Th/ ^{234}U/ ^{238}U$ and radiocarbon age measurements, and the suitable range of sample ages available in our cores. Our offshore core collections from Barbados, Kiritimati, and other Caribbean sites

contain hundreds of meters of core and thousands of pristine coral specimens between 4000 and 50,000 yr BP. Although it is our intention to quadruple the number of paired radiocarbon and $^{230}Th/ ^{234}U/ ^{238}U$ measurements over the next 3 years, the broad utility of our existing calibration data and the many active research programs spanning the past 50,000 yr BP years justifies their publication at this time.

2.2. Sample and data quality control

The Barbados and Kiritimati samples that are younger than 30,000 yr BP resided exclusively in the marine environment and are remarkably well preserved. There is little microscopic (petrographic, scanning electron microscope, or binocular) or mineralogical evidence of aragonite or high magnesium marine cements in the coral pore spaces, as is occasionally reported at other reef core sites (Ribaud-Laurenti et al., 2001; Paterne
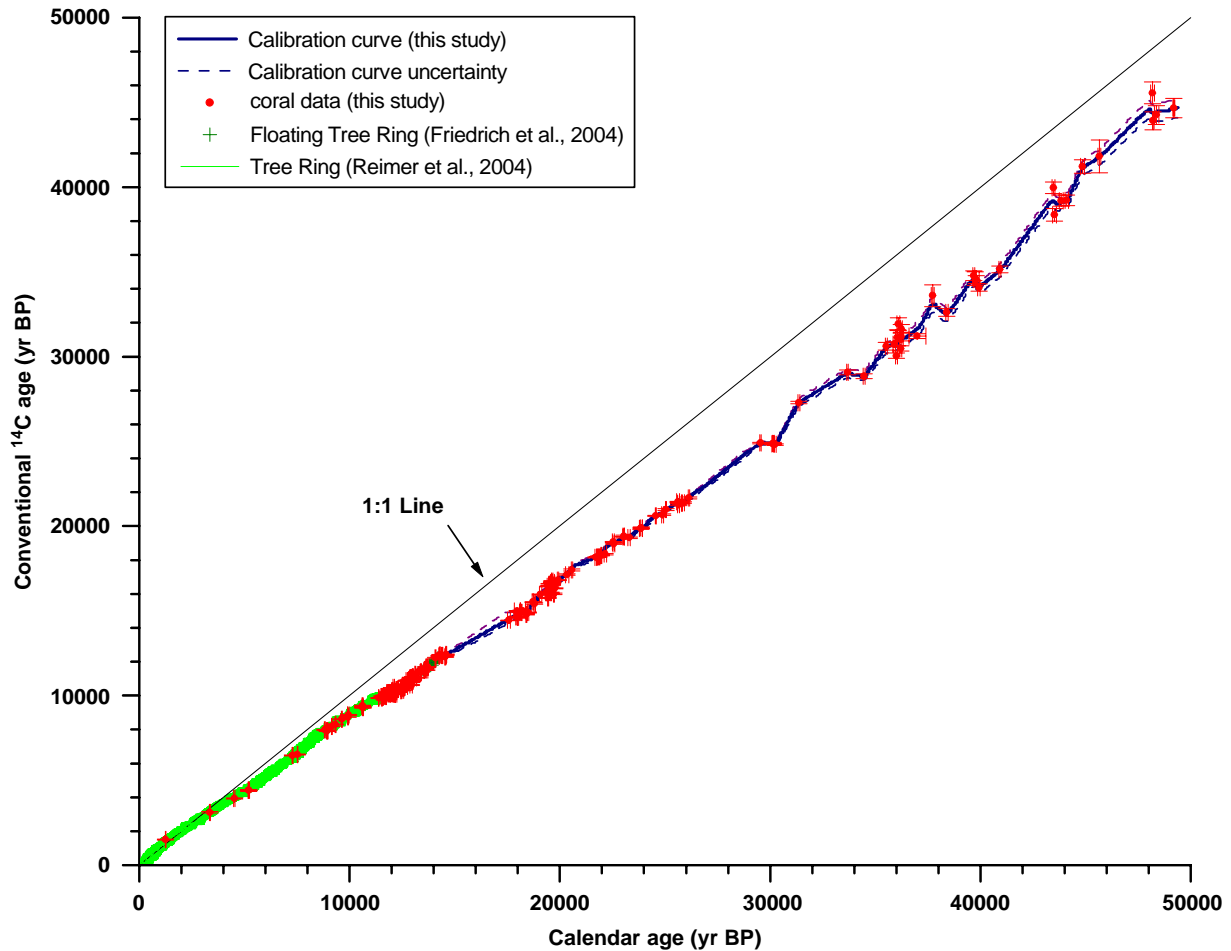
Fig. 3. Our coral calibration curve plotted with 1% confidence limits (corresponds to 3σ uncertainties for normal distributions) and coral data plotted with 1σ error bars. Calibration curve is compared to the tree ring chronologies (Reimer et al., 2004; Friedrich et al., 2004).

et al., 2004). The general lack of marine cements is probably due to the well ventilated locations of the Barbados and Kiritimati core sites, which are removed from tidal or evaporative tidal conditions. Any sample showing even trace amounts of marine cement was not analyzed. For all of our samples, we use a "less than 0.2% calcite" quality control criterion. Calcite content is measured using an X-ray diffraction instrument with a calibrated detection limit of 0.2% calcite in an aragonitic coral. These pristine drill core samples and rigorous quality control criteria for vadose (zone exposed to percolating rain water) exposed samples are especially essential to the accuracy of the older radiocarbon dates, where a trace amount of calcite (i.e., greater than 0.2%) can result in unacceptably large offsets in radiocarbon ages (Chiu et al., 2004, 2005). The "less than 0.2% calcite" is the single most important screening criterion we have adopted, and it explains many of the differences between our calibration curve and published coral data that typically use 1% calcite detection limits and measure between 1% and 5% calcite in their samples (Yokoyama et al., 2000; Paterne et al., 2004).

The rapid burial of these corals minimizes the potential for microboring and encrusting organisms to degrade the sample quality, such as has occurred with dredged samples that resided on the sea floor for tens of thousands of years (Paterne et al., 2004). Most Barbados samples older than 30,000 yr. were subaerially exposed during the last glacial maximum lowstand, but have remained below sea level for the past 14,000 yr. A few samples older than 30,000 yr grew in deep water and were not subaerially exposed during the subsequent glacial maximum lowstand. In addition to these samples, we analyzed surface outcrop samples from interstadial uplifted reefs on Araki Island (15.63°S; 166.93°E) in the southwest Pacific for the time interval from 33,000 to 50,000 yr BP (Urmos, 1985). All Araki samples were subaerially exposed and were rigorously examined for signs of diagenesis based on criteria described later in this paper. Importantly, none of the samples has been exposed to the corrosive effects of a freshwater (phreatic) lens that is deleterious to $^{230}Th/\ ^{234}U/\ ^{238}U$ dating accuracy (Hamelin et al., 1991).

The following is a list of specific sample screening and data quality control criteria that we use for the construction of our radiocarbon calibration. The detailed analytical methods, acceptable precision, and accuracy of U-series and radiocarbon analyses for inclusion in the calibration data set will be discussed in the methods sections.

- X-ray diffraction (XRD) measurements on each sample must indicate less than 0.2% calcite based on a documented 0.2% calcite or better detection limit. Calibration standards of varying percentages of calcite in an aragonite sample are run with each batch of samples.
- The [U] of corals must be within the range of living/modern samples taking into consideration the species and the correlation of [U] and calcification temperature (Min et al., 1995).
- The $\delta^{234}U_{initial}$ of coral samples must be between 138 and 150 per mil. Although the $\delta^{234}U$ of modern seawater and corals averages 146 (Delanghe et al., 2002; Cutler et al., 2004), the glacial $\delta^{234}U_{initial}$ estimates are slightly lower than this value (Cutler et al., 2004; Hughen et al., 2004a, b) and therefore, we have skewed the acceptable range toward lower values. Cutler et al. (2004) provides an analysis of the shifting $\delta^{234}U$ over time.
- After ultrasonic cleaning, samples are examined microscopically for any evidence of foreign particles or aragonite cements. Samples are rejected if they show aragonite cements or visible contamination that cannot be ultrasonically removed.
- U-series and radiocarbon samples are taken from 2 concentric cores drilled into 4 mm thick slabs of the coral samples with the radiocarbon sample taken from the inner core. This assures systematic sampling and cleaning procedures and the proximal location of the two age determinations. X-ray diffraction samples are taken from the outer "donut" sampled for the U-series dates and the remainder of the sub-sample is archived. For samples older than 20,000 yr BP, the inner core is subjected to an extended hydrogen peroxide pretreatment step in order to remove organic matter (Chiu et al., 2005).
- Radiocarbon measurements are made with a relative precision better than or equal to $+0.4\%$ (one sigma) for samples less than 30,000 years old.
- $^{230}Th/$ $^{234}U/$ ^{238}U age determinations are measured with a precision of better than $+3.0$ per mil (one sigma) over the entire calibration.
- A representative sampling of corals older than 30,000 yr BP that have been exposed to the vadose freshwater environment during the last glacial maximum low sea level, are analyzed for $^{231}Pa/$ ^{235}U ages, in addition to $^{230}Th/$ $^{234}U/$ ^{238}U ages, and ^{14}C ages in order to validate the $^{230}Th/$ $^{234}U/$ ^{238}U age

determinations (Mortlock et al., 2004; Chiu et al., 2005c).
- Coral samples are ranked according to the following scale, and we strive to obtain the highest Category samples available for a given interval. Our ultimate goal is to construct a calibration curve that utilizes only Categories I thru IV samples, with as many Category I & II samples as possible. Category III samples are used only where sea-level variations limit the possibility of collecting Category I & II samples.

  Category I. This category is reserved for samples that resided exclusively in the marine environment and have replicate radiocarbon and replicate $^{230}Th/$ $^{234}U/$ ^{238}U age measurements that fall within 2σ error respectively. Sample $^{230}Th/$ $^{234}U/$ ^{238}U ages are in stratigraphic order with respect to relative depth in core.

  Category II. Samples that resided exclusively in the marine environment and are either not replicated or not replicated to within 2σ. Sample $^{230}Th/$ $^{234}U/$ ^{238}U ages are in stratigraphic order with respect to their depth in core.

  Category III. Samples that were exposed to vadose (rainwater percolating zone) freshwater and have $^{231}Pa/$ ^{235}U and $^{230}Th/$ $^{234}U/$ ^{238}U ages that agree within 2σ error.

  Category IV. Samples that were that exposed to vadose freshwater and dated by $^{230}Th/$ $^{234}U/$ ^{238}U only.

  Category V. Samples that were exposed to the freshwater table (phreatic lens) and have $^{231}Pa/$ ^{235}U and $^{230}Th/$ $^{234}U/$ ^{238}U ages that agree within 2σ error.

  Category VI. Samples that were exposed to the phreatic lens and are not validated by concordant $^{230}Th/$ $^{234}U/$ ^{238}U and $^{231}Pa/$ ^{235}U dates.

2.3. $^{230}Th/$ $^{234}U/$ ^{238}U dating methods

We have developed techniques to determine the $^{230}Th/$ $^{234}U/$ ^{238}U and $^{231}Pa/$ ^{235}U ages in a single coral fragment by Multi-Collector Inductively Coupled Mass Spectrometry (MC-MS-ICPMS) (Mortlock et al., 2004) using fragments as small as 0.5 g. In the case where only U and Th measurements are required, the procedure is modified from the version presented in Edwards et al. (1987a). Only samples exposed to vadose freshwater will likely benefit from the redundant $^{231}Pa/$ ^{235}U measurement (Mortlock et al., 2004). Although the details of the U-series methodology are presented elsewhere (Mortlock et al., 2004), we repeat some of the important features of the instrumentation and methods here.

2.4. Mass spectrometry

U and Th isotopic measurements are made using our Fisons PLASMA 54 multi-collector magnetic sector double focusing Inductively Coupled Mass Spectrometer (MC-MS-ICPMS). A detailed description of the instrument design can be found elsewhere (Walder and Freedman, 1992; Halliday et al., 1995, 1998). In general, the instrument combines a double focusing magnetic sector mass spectrometer with an ICP source. Only a few of these instruments were manufactured, generally for the nuclear industry, and they varied in their configurations. Our instrument is equipped with a nine-collector Faraday array and is configured with an additional 30-cm radius Electro Static Analyzer (ESA) filter and a Daly detector with ion-counting capability. The abundance sensitivity achieved with the additional ESA energy filter is less than 0.3 ppm (measured as the contribution of mass 238 to mass 237 signal).

The sample injection into an ICP source is markedly simpler than loading a sample onto a filament and coaxing its ionization in a TIMS instrument. We employ either a MCN6000 desolvating nebulizer (CETAC) fitted with a PFA spray chamber or the ARIDUS 1 (PFA), fitted with a $50 \mu l/min$ PFA micro nebulizer (Elemental Scientific Inc.) Typical sensitivity for our instrument is about 0.4 pA per ppb for ^{238}U. Ionization efficiencies (the ratio of atoms detected to atoms introduced) for U, Th, and Pa are about a factor of 5–10 lower than those reported by TIMS. However, the routine precision in isotope ratios by MC-MS-ICPMS is comparable to the most precise measurements made by TIMS and the simplified sample injection and resulting increase in sample throughput present distinct advantages for the MC-MS-ICPMS technique. Fortunately in the case of corals, sample size is never a limitation.

The precise determination of isotopic ratios of U, Th, and Pa requires that mass fractionation (bias) and gain efficiency (calibration of the Daly detector) be known. Since the ion beam produced by a plasma source is relatively unstable, both fractionation and gain corrections must be made during the analyses. In order to make real-time corrections for mass bias, gain correction, and beam instability, we employ a multi-static routine for each U, Th, and Pa analysis. This approach is similar to that described in Luo et al. (1997) where it was demonstrated that multi-static routines yielded superior analytical precision for U and Th isotopic analyses. All measurements of the minor abundance isotopes (^{229}Th, ^{230}Th, ^{232}Th, ^{231}Pa, ^{233}Pa, ^{233}U, ^{234}U, ^{235}U) are made with the Daly Detector and are accompanied by simultaneous measurement of ^{238}U using one of the Faraday cups. Accurate gain corrections of the $^{233}U/^{238}U$ and $^{234}U/^{238}U$ isotope ratios require that the Daly detector operate without intensity biasing. Gain corrections of the $^{229}Th/^{230}Th$, $^{229}Th/^{232}Th$, and $^{233}Pa/^{231}Pa$ ratios are eliminated because the individual isotopes measured on the Daly detector are all normalized to ^{238}U. Measurement precision of the U and Th isotope ratios (about 75 and 60 ratio measurements, respectively) are generally better than $\pm 0.08\%$ and $\pm 0.3\%$ (2 RSD) respectively. This translates to an average uncertainty of about 0.5% (2 RSD) of the age for the $^{230}Th/^{234}U/^{238}U$.

2.5. Radiocarbon methods

At LLNLs subsamples of fossil corals are coarsely crushed, sonicated in Milli-Q water, the Milli-Q is decanted, the samples are dried, and weighed. An appropriate amount of 0.1 N HCl is added to the coral sample to remove 50–60% of the material (Yokoyama et al., 2000). Samples older than 30,000 yr receive a 60% leach. The neutralized acid and related salts are decanted, and the coral material is rinsed repeatedly with Milli-Q water and subsequently dried on a heating block. All radiocarbon samples older than 32,000 yr BP were ultrasonically cleaned in 30% hydrogen peroxide for seven days in order to oxidize any mold or other extraneous organic matter (including possible soil contamination) and analyzed at Leibniz-Labor for Radiometric Dating and Isotope Research at Christian-Albrechts University Kiel. In the Leibniz-Labor, the samples were subjected to a 60% leach with 1% HCl at room temperature overnight, followed by washing with Milli-Q water and a 15 min treatment with 15% hydrogen peroxide. The peroxide was siphoned off and the dampened samples were loaded directly into the vacuum extraction system to shield the sample from contamination with atmospheric CO_2.

At LLNL, approximately 20 mg samples, an appropriate amount to yield 1.0 mg-carbon targets, are placed in glass tubes and evacuated to 1×10^{-3} Torr with gentle heating. A 0.5 ml aliquot of 85% phosphoric acid is injected into the glass tubes, and the tubes are placed on a heating block at $90 °C$. The CO_2 that is released via this process is extracted through an offline manifold, cryogenically purified to remove water, and transferred into individual graphite reduction reactors. Similar to the procedure of Vogel et al. (1987), the CO_2 is reduced to graphite at $570 °C$ in the presence of an iron catalyst and a stoichiometric excess of hydrogen. The graphite is then transferred and pressed into aluminum target holders for subsequent analysis by accelerator mass spectrometry.

At Leibniz-Labor, the procedure is largely the same as at LLNL (Nadeau et al., 2001), except that 100% phosphoric acid is used, and is evacuated separately during heating, and then vented with nitrogen. Carbonate and acid are then evacuated together, sealed in a glass ampoule and reacted overnight in a water bath at $90 °C$. The reduction is done at $600 °C$.

At LLNL, the prepared graphite targets are sputtered in a high-intensity cesium sputter source (Southon and Roberts, 2000) with an equivalent ^{12}C- current of 275–300 μA, which yields 900–1000 ^{14}C counts/second on a modern carbon sample. After mass selection via the low energy injector magnet, the negative ion beam (^{13}C- or ^{14}C- and molecular isobars) is injected into the accelerator (FN Tandem Van de Graaff at CAMS), passed through a stripper foil and, on exiting the accelerator, is magnetically and velocity filtered and subsequently measured in an off-axis Faraday cup ($^{13}C^{4+}$) or analyzed in a gas ionization detector ($^{14}C^{4+}$) (Davis et al., 1990). The CAMS ion source sample wheel has slots for up to 64 targets and normally about 50 unknown samples are loaded in a routine sample wheel. Each wheel load is composed of a suite of primary (OX1) and secondary (OX2, ANU, TIRI wood) standards and the unknown samples, and is broken into several groups. In general, a group is composed of two sub-groups containing 5–7 targets with intervening and bracketing primary standards. Samples are analyzed in such a fashion that a single group is completely analyzed prior to proceeding on to the next group. A group is analyzed repeatedly such that a suite of bracketing blanks, primary standards, and secondary standards are analyzed in conjunction with the unknown samples. A single group of unknowns is cycled through at least five times. During each cycle, an individual target is analyzed for either 30,000 ^{14}C events or 200 s, whichever comes first.

At LLNL, raw data ($^{14}C/$ ^{13}C ratios) are normalized to the average of the bracketing six primary standards for each pass through a sample group. Counting errors (primary standard and unknown) are propagated through the analysis and are assumed to be Gaussian (Bevington and Robinson, 1992). The average of the n-measurement-cycles of each unknown is then determined and for the initial error, the larger of the counting error or the external error of the n-cycles is chosen. CAMS ^{14}C dates are based on $^{14}C/$ ^{13}C atom ratios, not decay counting to obtain specific ^{14}C activities. The algorithms used at CAMS (Southon, unpublished) are similar to those developed at Arizona (Donahue et al., 1990). Radiocarbon age data are presented according to the conventions of Stuiver and Polach (1977) using the Libby half-life (5568 yr.). The Δ ^{14}C calculations are made based on the more recent ^{14}C half-life of 5730 ± 40 years (Godwin, 1962). Calculations include a background subtraction based on measurements of a fossil coral and inclusion of background error based on ^{14}C-free calcite determined on multiple aliquots of acid leached calcite for each wheel of unknowns (cf. Brown and Southon, 1997).

Twenty-eight unleached aliquots of TIRI turbidite were analyzed with our LLNL AMS ^{14}C measurements over a time span of 18 months. Individual analyses ranged from 18090 to 18245 yr BP with reported one standard deviation errors between 30 and 50 years. The weighted average Fraction Modern of these 28 measurements shows a one standard deviation scatter of 0.00044 (±35 years). The weighted mean and weighted mean uncertainty (one-sigma) of the TIRI turbidite results are 0.10378 ± 0.00008 ($n=24$) that equates to $18,199\pm8$ years. The fractional error of these results indicates reproducibility of individual measurements at the 4 per mil (one sigma) level, which is consistent with the quoted counting statistics errors.

Samples older than 32,000 years were measured at the Leibniz-Labor for Radiometric Dating and Isotope Research at the Christian-Albrechts University Kiel (Nadeau et al., 1997, 1998). The model 846B HVEE cesium sputter ion source was run at moderate outputs around 30 μA equivalent $^{12}C^-$ beam for optimal stability, giving around 60 counts/s for a modern sample. The separator/recombinator selects masses 12, 13, and 14, attenuates mass 12 by a factor 100, and injects the three masses simultaneously into the HVEE 3 MV tandem accelerator at 2.5 MV. $^{12}C^{+3}$ and $^{13}C^{+3}$ are measured simultaneously in two off-center Faraday cups, and $^{14}C^{+3}$, after electrostatic deflection and a 90° magnet, in a gas ionization detector, yielding both $^{14}C/$ ^{12}C and $^{13}C/$ ^{12}C ratios simultaneously. These ratios are largely insensitive to fluctuations in ion source output or transmission. The 846B wheel loads about 40 unknowns together with 8 OXII standards, backgrounds and reference materials spaced evenly between the unknowns. Stable and reproducible target preparation and measuring conditions make it possible to use the average of all OXII targets for comparison with the unknowns in each cycle. Comparison of the scatter statistics between cycles with Poisson statistics indicates Poisson statistics is the main cause of the measuring uncertainty (Nadeau et al., 1998). "Old" coral samples are used to provide the optimum background subtraction (Nadeau et al., 2001). The blank value for Araki coral AK-H-2 was 0.1334 ± 0.0114 pMC (average of 5 targets). This scatter-based uncertainty is unusually small, so we adopted a more conservative and conventional value of 1/8 of the blank (0.0167) as its uncertainty. The $^{230}Th/$ ^{234}U age of AK-H-2 is 97,000 yr BP.

2.6. Barbados, Kiritimati and Araki reservoir age estimates

The radiocarbon content of tropical surface water is depleted in ^{14}C compared to the atmosphere due to incomplete isotopic equilibration and mixing with subsurface waters of older ages. This ^{14}C offset between surface water and atmosphere is known as the "reservoir age" and in recent times ranges between 300 and 500 years in the western tropical and subtropical regions

between 40N and 40S (Craig, 1957; Stuiver and Polach, 1977; Bard 1988). Fairbanks (1989) used a reservoir age of 400 years for Barbados radiocarbon ages based on an average of data for the western tropical Atlantic summarized in Bard (1988). In this paper, we compute the reservoir age for Barbados, Kiritimati, and Araki coral samples dated by $^{230}Th/$ $^{234}U/$ ^{238}U and ^{14}C by subtracting the coral ^{14}C ages from the tree ring radiocarbon calibration curve (Reimer et al., 2004). The results are plotted in Fig. 2. There is an advantage to computing an average reservoir age from data spread over the Holocene, rather than from only a few measurements of preindustrial ages. The application of a Holocene reservoir age to older time periods is only an assumption; however, by selecting sites in the western Atlantic and central and western Pacific, we have some assurance that surface waters at Barbados, Kiritimati, and Araki were not exposed to newly upwelled waters deficient in ^{14}C. It is possible that large and rapid ^{14}C concentration changes may have resulted in large transient increases in the difference between atmosphere and surface ocean waters that could last decades or even centuries. More importantly, the uncertainty in the reservoir age in samples older than the Holocene becomes less significant as the analytical age uncertainties in radiocarbon and $^{230}Th/$ $^{234}U/$ ^{238}U ages increase with time. The computed reservoir ages are remarkably similar: Barbados $= 365 \pm 60$ years ($n = 21$); Kiritimati $= 350 \pm 55$ years ($n = 4$); and Araki $= 365 \pm 140$ years ($n = 9$). Whereas additional measurements are needed to reduce the uncertainty of these reservoir ages, we believe that most of the variability is due to the high frequency fluctuations produced in the atmosphere that are attenuated in the surface ocean. In other words, the reported uncertainties in the reservoir ages do not reflect the natural variability in the local reservoir ages at these three sites (Appendix A).

2.7. Methodology of the radiocarbon calibration 0 to 50,000 yr BP

Our $^{230}Th/$ $^{234}U/$ ^{238}U radiocarbon calibration is intended as a stand-alone radiocarbon calibration that spans 0–50,000 yr BP and is based on our most stringent sample quality criteria. At this time, we see no benefit in amalgamating subsets of calibration points from other data sets based on the dramatic increase in scatter when we include data from other coral, varved-sediment, and speleothem calibration curves. Even the Cariaco (Hughen et al., 2000, 2004b) varved sequence seems to be offset between 13,300 and 14,000 yr BP compared to the floating tree ring chronology of Friedrich et al. (1999, 2001, 2004) and our coral data (Fig. 2). Most importantly, we believe that only calibration data points that have independent and quantifiable precision and accuracy error estimates for radiocarbon and calendar

ages are suitable for inclusion in any calibration curve. The pristine nature of our coral samples, data density, the fact that from 10,000 to 29,000 yr BP all of our samples have resided exclusively in the marine environment, our level of sample documentation, consistency of sample screening, handling, and analysis, and the precision of our measurements justify a stand-alone calibration curve that can be compared to many other independently determined curves. Sample selection criteria for inclusion in our calibration are more stringent than IntCal04 (Reimer et al., 2002, 2004) or Marine04 (Hughen et al., 2004) and are based on the sample quality Categories described above, and only samples that have been submerged in seawater are included unless subaerially exposed samples are the only available samples for a given time interval. Ultimately, we expect our calibration curve will include mostly samples submerged in seawater since growth, where coral aragonite is thermodynamically stable. Although we choose not to amalgamate our data with other calibration data in this paper, we are actively participating in combining our radiocarbon calibration data in international calibration efforts using a subset of our samples younger than 26,000 yr BP (Reimer et al., 2004; Hughen et al., 2004b) and in ice core age model development and $\Delta^{14}C$ reconstructions combining our older samples with data from other groups (e.g., Shackleton et al., 2004).

One can make the argument that the calibration of a radiocarbon age is only as good as the precision, accuracy, and proximity of the pair(s) of coral calibration data points that bracket the radiocarbon date, because all errors are independent. The prime disadvantage of this simple approach is that errors in the calibration data occur in both calendar ($^{230}Th/$ $^{234}U/$ ^{238}U) and radiocarbon measurements, and therefore, it is not a simple matter to rigorously estimate the error bars on the calibrated radiocarbon ages. The tree ring calibration routine (Stuiver et al., 1998b) and INTCAL98 (Stuiver et al., 1998a) assume that there is no error in tree ring calendar ages or coral $^{230}Th/$ ^{234}U ages, so they obviate this problem entirely, regardless of whether an 11,900 composite tree ring calibration or corals have calendar age uncertainties. More recently, IntCal04 (Reimer et al., 2004) and Marine04 (Hughen et al., 2004) calibration curves have adopted a more rigorous treatment of errors in radiocarbon and calendar years (Buck and Blackwell, 2004).

A statistically more rigorous treatment of error estimates in the calibration curve (in both calendar years and radiocarbon years) and the means to convert radiocarbon ages and errors to calendar years requires a statistical model of moderate complexity. In the following section, we present a statistical model that permits rigorous error treatment in radiocarbon ages calibrated using our coral data set. We provide a radiocarbon

calibration program on our web site http://www.radio-carbon.LDEO.columbia.edu/ where our calibration curve can be accessed and where updates will be released. Our coral data sets and documentation are also archived at this web site.

2.8. Calibration procedure with error estimation based on a hierarchical bayesian statistical model

2.8.1. Calibration approach

Our main premise is that there exists a precise, deterministic functional relationship between the calendar age x and the radiocarbon age y

$$y = f(x).$$

This relationship is not known exactly, but it is assumed to be applicable to the true (unaffected by measurement errors) x and y of samples. Were f known, the calendar age x of a sample with the measured radiocarbon age y could be found by the inversion $x = f^{-1}(y)$ (possibly

with multiple values, because f is not necessarily monotonous). Error bars or a given error distribution for y could be converted easily to those for x as well.

Because the precise form of $y = f(x)$ is not known, we attempt to develop its statistical description. The complete description would be a joint probability density of values $f(x)$ for all x's. However, here we only consider a problem of a single-sample calibration (as opposed to sets of samples with a priori information on their time sequence, e.g., Buck et al., 1996; Steier et al., 2001; Bronk Ramsey, 2001); hence, it will suffice to obtain marginal distributions for individual values of x. More precisely, we will only compute the function $p_c(y,x) = p(y|x)$, that for each given x expresses the density of probability with which $f(x)$ may take value y (shown by colors in Fig. 4). Indeed, when this probability distribution is available, Bayes' formula provides an easy way to compute the distribution of the calendar age for an individual sample, given the measurement of its radiocarbon age y_m and the
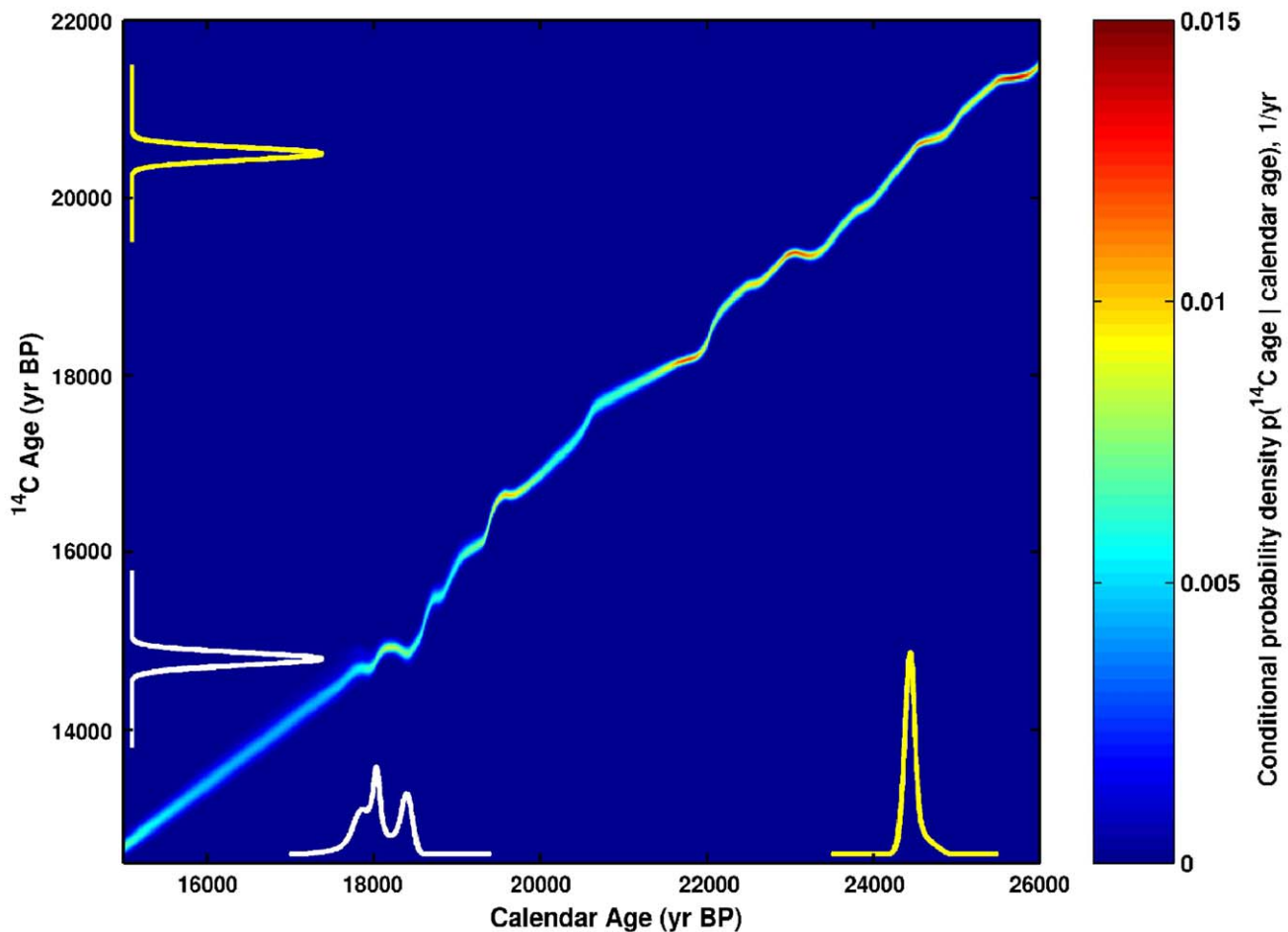
Fig. 4. Plot is an example of the conditional probability density function for ^{14}C age given the calendar age for the calendar interval between 15,000 and 26,000 yr BP. Two examples of radiocarbon age inputs and calendar year output estimates illustrate a simple unimodel conversion case (yellow line) and an example where the calibration curve has a fluctuation producing a broad uncertainty and bimodality in estimated calendar age (white line). White and yellow curves show probability density functions in 1/yr, so their values are not in the scale of the color plot axes. The areas under all probability density curves are equal to 1. (See Appendix Table 1 in the online version of this article for detailed statistics).

Table 1
Typical examples of radiocarbon age conversion to calendar years using our calibration curve (Fig. 4)

	Mean	Median	Std
Example 1			
Radiocarbon age (raw) input:	14,800	14,800	70
Calendar age output:	18,114	18,090	257
	Mean	Median	Std interval
Example 2			
Radiocarbon age (raw) input:	20,500	20,500	70
Calendar age output:	24,533	24,510	116

distribution of the measurement error (Dehling and Van der Plicht, 1993):

$$p(x|y_m) = \frac{p(y_m|x)p_a(x)}{\int p(y_m|x)p_a(x)\,dx} \propto p(y_m|x)p_a(x), \qquad (1)$$

where p_a is the assumed prior distribution of the sample's calendar age (before the radiocarbon age measurement became known), e.g., a uniform distribution on the entire calibration period. It follows that,

$$p(y_m|x) = \int p(y_m|y)p(y|x)\,dy$$
$$= \int q(y_m - y)p_c(y, x)\,dy, \qquad (2)$$

where q is the probability density function of the radiocarbon age measurement error. Inserting (2) into (1) obtain

$$p(x|y_m) \propto p_a(x)\int q(y_m - y)p_c(y, x)\,dy, \qquad (3)$$

Fig. 4 shows examples of this conversion for the radiocarbon ages 14.8 K (white lines) and 20.5 K (yellow lines) when the radiocarbon age measurement error is assumed normally distributed with the standard deviation of 70 years (See Appendix Table 1 in the online version of this article for the statistics of the resulting distributions). Note the bimodal distribution of the calendar age produced by formula (3) in the former case, due to the non-monotonous behavior of the calibration curve.

2.8.2. General methodology

We use the hierarchical Bayesian modeling to estimate the conditional probability distribution function $p_c(y, c) = p(y|x)$. This uses two different stages to account for uncertainties in observations of x and y. The first stage computes the distribution $p(y|x)$ for a given set of samples on the basis of a given uncertainty in their radiocarbon ages under assumption of no error in their calendar ages. This stage uses least-squares estimation approach with an additional weak constraint on the local slope of the calibration curve. The solution

at this stage is similar to the linear smoothing spline approximation (Wahba, 1990) or "random-walk" calibration approaches (Gómez Portugal Aguilar et al., 2002). The second stage of the hierarchical modeling uses the Monte Carlo approach for simulating the observational uncertainty in calendar ages of all samples: each member of this ensemble has its own realization of calendar ages for all samples, so the computation of the first stage is repeated for each ensemble member, and the corresponding marginal distribution $p(y|x)$ for each member is produced. The final solution is obtained by averaging the marginal distributions $p(y|x)$ over all members of the entire Monte Carlo ensemble.

2.8.3. Implementation details

In the practical implementation of this procedure, the grids of x and y were discretized for the 10 year resolution. The original multiple measurements of x and y were reduced to a single pair of x and y for each sample using an optimal averaging procedure. A χ^2-based quality control procedure was used to prune out samples with inconsistent individual measurements, reducing the total number of samples from 154 to 152. Further consistency checks resulted in the uniform inflation of all measurement error estimates by the factors of 1.8 and 1.3 for the calendar and radiocarbon standardized errors respectively. An analysis of linear interpolation lines computed for a preliminary Monte Carlo ensemble (size 1000) of the entire set of 152 data points perturbed by simulated measurement errors was used to derive a priori estimates necessary for our procedure: expected slope changes from point to point, slope uncertainty (assumed normal with 0.8 yr/yr standardized deviation), and the age variability inside 10 year grids. The Monte Carlo ensemble of 4000 was used for obtaining the final solution (Figs. 3 and 4).

2.8.4. Description of the calibration curve

The offset between radiocarbon years and calendar years increases from the present to approximately 38,500 calendar years BP reaching more than 6000 years difference. From 38,500 calendar years BP to 50,000 calendar years BP the trend reverses and radiocarbon ages grow slightly closer to calendar ages (Fig. 3). By 50,000 calendar years BP, the corresponding radiocarbon age is younger by approximately 3700 years. The departure of the calibration curve from the one to one line (Δ ^{14}C) contains fundamental information on solar output (Damon et al., 1978; Stuiver and Quay, 1980), the carbon cycle (Edwards et al., 1993; Hughen et al., 1998; Hughen et al., 2000), and the Earth's geomagnetic field (Bard et al., 1990; Beck et al., 2001). The overall shape of our calibration curve corresponds to the broad scale changes in the Earth's geomagnetic field intensity, but the magnitude of the

radiocarbon and calendar year offset is apparently too large to be explained by magnetic field intensity changes alone (Beck et al., 2001; Hughen et al., 2004a). Box model calculations of the radiocarbon production history computed as a function of estimated changes in the Earth's geomagnetic field intensity (Laj et al., 2000, 2004) show a sharp increase between 50,000 and 40,000 yr BP, followed by a gradual decrease between 35,000 yr BP and the present. The sharp decrease between 50,000 and 40,000 yr BP corresponds to the transition between Earth's field strength comparable to today's to the peak of the Laschamp geomagnetic excursion when Earth's geomagnetic field intensity nearly collapsed. Measurements of ^{10}Be and ^{36}Cl spikes in ice cores mark the Laschamp cosmogenic isotope production signal in the atmosphere (Beer et al., 1988). However, due to the brevity of the Laschamp excursion and the attenuation of the atmospheric ^{14}C anomaly through ocean mixing, there is no dramatic radiocarbon age anomaly corresponding to the peak Laschamp event.

A possible additional explanation for the growing offset between radiocarbon years and calendar years is an inaccurate radiocarbon decay constant (Godwin, 1962). In general, higher precision and higher accuracy radioisotope data measured by mass spectrometry techniques have outgrown the lower precision and lower accuracy decay constants measured many decades ago by decay-counting methods (Renne et al., 1998; Cheng et al., 2000). A more accurate and precise measurement of the radiocarbon decay constant is required before we can quantify the role of the sun, carbon cycle, and the geomagnetic field in distorting the radiocarbon time-scale. If the measured offset between radiocarbon years and calendar years were explained by Earth's geomagnetic field intensity alone, it requires a decrease in the radiocarbon decay constant by several percent below the adopted value (Godwin, 1962).

3. Conclusions

Paired radiocarbon and ^{230}Th/ ^{234}U/ ^{238}U age determinations on pristine corals provide a high precision, high accuracy radiocarbon calibration curve suitable for general use beyond the limits of the superior tree ring calibration curve (Stuiver et al., 1998a; Reimer et al., 2004). Results presented in this paper overlap with the existing tree ring calibration curve and extend the calibration to 50,000 yr BP. Our calibration curve can be used to convert radiocarbon ages to calendar ages with an online conversion program http://www.radio carbon.LDEO.columbia.edu/ that includes a rigorous error estimation.

Appendix A. Electronic Supplementary Material

The online version of this article contains additional supplementary data. Please visit doi:10.1016/j.quascirev.2005.04.007.

References

Andersen, K.K., Azuma, N., Barnola, J.-M., et al., 2004. High-resolution record of Northern Hemisphere climate extending into the last interglacial period. Nature 431 (7005), 147–151.

Arnold, J.R., Libby, W.F., 1949. Age determinations by radiocarbon content: Checks with samples with known age. Science 110, 678–680.

Bard, E., 1988. Correction of accelerator mass spectrometry ^{14}C ages measured in planktonic foraminifera: paleoceanographic implications. Paleoceanography 3 (6), 635–645.

Bard, E., 1998. Geochemical and geophysical implications of the radiocarbon calibration. Geochimica et Cosmochimica Acta 62 (12), 2025–2038.

Bard, E., Hamelin, B., Fairbanks, R.G., Zindler, A., 1990. Calibration of the ^{14}C timescale over the past 30,000 years using mass spectrometric U-Th ages from Barbados corals. Nature 345, 405–410.

Bard, E., Arnold, M., Fairbanks, R.G., Hamelin, B., 1993. ^{230}Th/^{234}U and ^{14}C ages obtained by mass spectrometry on corals. Radiocarbon 35 (1), 191–199.

Bard, E., Arnold, M., Hamelin, B., Tisnerat-Laborde, N., Cabioch, G., 1998. Radiocarbon calibration by means of mass spectrometric ^{230}Th/ ^{234}U and ^{14}C ages of corals: an updated database including samples from Barbados, Mururoa and Tahiti. Radiocarbon 40, 1085–1092.

Beck, J.W., Richards, D.A., Edwards, R.L., Silverman, B.W., Smart, P.L., Donahue, D.J., Herrera-Osterheld, S., Burr, G.S., Calsoyas, L., Jull, A.J.T., Biddulph, D., 2001. Extremely large variations of atmospheric ^{14}C concentration during the last glacial period. Science 292, 2453–2458.

Beer, J., Siegenthaler, U., Bonani, G., Finkel, R.C., Oeschger, H., Suter, M., Wolfli, W., 1988. Information on past solar activity and geomagnetism from ^{10}Be in the C amp Century ice core. Nature 331, 675–679.

Bevington, P.R., Robinson, D.K., 1992. Data reduction and error analysis for the physical sciecnes 2nd edition. McGraw-Hill, New York, USA 328p.

Bronk Ramsey, C., 2001. Development of the radiocarbon calibration program. Radiocarbon 43, 355–363.

Brown, T.A., Southon, J.R., 1997. Corrections for contamination background in AMS ^{14}C measurements. Nuclear Instruments and Methods in Physics Research B 123, 208–213.

Buck, C.E., Blackwell, P.G., 2004. Formal statistical models for estimating radiocarbon calibration curves. Radiocarbon 46, 1093–1102.

Buck, C.E., Cavanagh, W.G., Litton, C.D., 1996. Bayesian Approach to Interpreting Archaeological Data. John Wiley & Sons, Chichester, New York, Brisbane, Toronto, Tokyo, Singapore 382p.

Burr, G.S., Beck, J.W., Taylor, F.W., Recy, J., Edwards, R.L., Cabioch, G., Correge, T., Donahue, D.J., O'Malley, J.M., 1998. A high-resolution radiocarbon calibration between 11,700 and 12,400 calendar years BP derived from ^{230}Th ages of corals from Espiritu Santo Island, Vanuatu. Radiocarbon 40, 1093–1105.

Chen, J.H., Edwards, R.L., Wasserburg, G.J., 1986. ^{238}U, ^{234}U, and ^{230}Th in seawater. Earth and Planetary Science Letters 80, 241–251.

Cheng, H., Edwards, R.L., Hoff, J., Gallup, C.D., Richards, D.A., Asmerom, Y., 2000. The half-lives of uranium-234 and thorium-230. Chemical Geology 169, 17–33.

Chiu, T.-C., Fairbanks, R.G., Mortlock, R.A., 2004. Radiocarbon calibration between 30,000 and 50,000 years before present using fossil corals. AUG ann. mting., abstr.

Chiu, T.-C., Fairbanks, R.G., Mortlock, R.A., Bloom, A.L., 2005. Extending the radiocarbon calibration beyond 26,000 years before present using fossil corals, Quaternary Science Reviews, this issue, doi:10.1016/j.quascirev.2005.04.002.

Craig, H., 1957. The natural distribution of radiocarbon and the exchange time of carbon dioxide between atmosphere and sea. Tellus 9 (1), 1–17.

Cutler, K.B., Gray, S.C., Burr, G.S., Edwards, R.L., Taylor, F.W., Cabioch, G., Beck, J.W., Cheng, H., Moore, J., 2004. Radiocarbon calibration and comparison to 50 kyr BP with paired ^{14}C and ^{230}Th dating of corals from Vanuatu and Papua New Guinea. Radiocarbon 46, 1127–1160.

Damon, P.E., 1988. Production and decay of radiocarbon and its modulation by geomagnetic field-solar activity changes with possible implications for global environment. In: Stephenson, F.R., Wolfendale, A.W., (Eds.), Secular Solar and Geomagnetic Variations in the Last 10,000 years: NATO ASI Series. Series C. Academic Publishers, Dordrecht; Boston, Kluwer Academic Publishers, pp. 267–285.

Damon, P.E., Long, A., 1962. Arizona radiocarbon dates III. Radiocarbon 4, 239–249.

Damon, P.E., Long, A., Sigalove, J.J., 1963. Arizona Radiocarbon Dates IV. Radiocarbon 5 (1), 283–301.

Damon, P.E., Lerman, J.C., Long, A., 1978. Temporal fluctuations of atmospheric ^{14}C: causal factors and implications. Annual Review of Earth and Planetary Sciences 6, 457–494.

Dansgaard, W., White, J.W.C., Johnsen, S.J., 1989. The abrupt termination of the Younger Dryas climate event. Nature 339, 532–534.

Dansgaard, W., Johnsen, S.J., Clausen, H.B., Dahl-Jensen, D., Gundestrup, N.S., Hammer, C.U., Hvidberg, C.S., Steffensen, J.P., Sveinbjornsdottir, A.E., Jouzel, J., Bond, G., 1993. Evidence for general instability of past climate from a 250-Kyr ice-core record. Nature 364, 218–220.

Davis, J.C., Proctor, I.D., Southon, J.R., Caffee, M.W., Heikkinen, D.W., Roberts, M.L., Moore, T.L., Turteltaub, K.W., Nelson, D.E., Loyd, D.H., Vogel, J.S., 1990. LLNL/UC AMS facility and research program. Nuclear Instruments and Methods in Physics Research B 52, 269–272.

Dehling, H., van der Plicht, J., 1993. Statistical problems in calibrating radiocarbon dates. Radiocarbon 35, 239–244.

Delaygue, G., Stocker, T.F., Joos, F., Plattner, G.-K., 2003. Simulation of atmospheric radiocarbon during abrupt oceanic circulation changes: trying to reconcile models and reconstructions. Quaternary Science Reviews 22, 1647–1658.

Delanghe, D., Bard, E., Hamelin, B., 2002. New TIMS constraints on the Uranium–238 and Uranium–234 in seawaters from the main ocean basins and the Mediterranean Sea. Marine Chemistry 80, 79–93.

de Vries, H., 1958. Variation in concentration of radiocarbon with time and location on Earth. Proceedings Koninklijke Nederlandse Akademie van Wetenschappen, Series B 61, 94–102.

de Vries, H., 1959. Measurement and use of natural radiocarbon. In: Abelson, P.H. (Ed.), Researches in Geochemistry. Wiley, New York, pp. 169–189.

Donahue, D.J., Linick, T.W., Jull, A.J.T., 1990. Isotope-ratio and background corrections for accelerator mass spectrometry radiocarbon measurements. Radiocarbon 32, 135–142.

Edwards, R.L., 1988. High-precision thorium-230 ages of corals and the timing of the sea level fluctuations in the late Quaternary. Ph.D. thesis, California Institute of the Technology.

Edwards, R.L., Chen, J.H., Wasserburg, G.J., 1987a. ^{238}U-^{234}U-^{230}Th-^{232}Th systematics and the precise measurement over the past 500,000 years. Earth and Planetary Science Letters 81, 175–192.

Edwards, R.L., Chen, J.H., Ku, T.-L., Wasserburg, G.J., 1987b. Precise timing of the last interglacial period from mass spectrometric determination of Thorium-230 in corals. Science 236, 1547–1553.

Edwards, R.L., Beck, J.W., Burr, G.S., Donahue, D.J., Chappell, J.M.A., Bloom, A.L., Druffel, E.R.M., Taylor, F.W., 1993. A large drop in atmospheric ^{14}C/^{12}C and reduced melting in the Younger Dryas, documented with ^{230}Th ages of corals. Science 260, 962–968.

Edwards, R.L., Cheng, H., Murrell, M.T., Goldstein, S.J., 1997. Protactinium-231 Dating of Carbonates by Thermal Ionization Mass Spectrometry: Implications for Quaternary Climate Change. Science 276, 782–786.

Elsasser, W., Ney, E.P., Winckler, J.R., 1956. Cosmic-ray intensity and geomagnetism. Nature 178, 1226–1227.

Fairbanks, R.G., 1989. A 17,000-year glacio-eustatic sea level record: influence of glacial melting rates on the Younger Dryas event and deep-ocean circulation. Nature 342, 637–642.

Fairbanks, R.G., 1990. The age and origin of the "Younger Dryas climate event" in Greenland ice cores. Paleoceanography 6, 937–948.

Friedrich, M., Kromer, B., Spurk, M., Hofmann, J., Kaiser, K.F., 1999. Paleo-environment and radiocarbon calibration as derived from Late Glacial/Early Holocene tree-ring chronologies. Quaternary International 61, 27–39.

Friedrich, M., Kromer, B., Kaiser, K.F., Spurk, M., Hughen, K.A., Johnsen, S.J., 2001. High-resolution climate signals in the Bølling-Allerød Interstadial (Greenland Interstadial 1) as reflected in European tree-ring chronologies compared to marine varves and ice-core records. Quaternary Science Reviews 20 (11), 1223–1232.

Friedrich, M., Remmele, S., Kromer, B., Hofmann, J., Spurk, M., Kaiser, K.F., Orcel, C., Kuppers, M., 2004. The 12,460-year Hohenheim oak and pine tree-ring chronology from central Europe—a unique annual record for radiocarbon calibration and paleoenvironment reconstructions. Radiocarbon 46, 1111–1122.

Gallup, C.D., Edwards, R.L., Johnson, R.G., 1994. The timing of high sea levels over the past 200,000 years. Science 263, 796–800.

Gallup, C.D., Cheng, H., Taylor, F.W., Edwards, R.L., 2002. Direct determination of the timing of the sea level change during termination II. Science 295, 310–313.

Godwin, H., 1962. Half-life of radiocarbon. Nature 195, 984.

Gómez Portugal Aguilar, D., Litton, C.D., O'Hagan, A., 2002. Novel statistical model for a piece-wise linear radiocarbon calibration curve. Radiocarbon 44, 195–212.

Goslar, T., Arnold, M., Tisnerat-Laborde, N., Czernik, J., Wieckowski, K., 2000a. Variations of Younger Dryas atmospheric radiocarbon explicable without ocean circulation changes. Nature 42, 877–880.

Goslar, T., Hercman, H., Pazdur, A., 2000b. Comparison of U-series and radiocarbon dates of speleothems. Radiocarbon 42 (3), 403–414.

Goslar, T., Arnold, M., Tisnerat-Laborde, N., Hatte, C., Paterne, M., Ralska-Jasiewiczowa, M., 2000c. Radiocarbon calibration by means of varves versus ^{14}C ages of terrestrial macrofossils from Lake Gosciaz and Lake Perespilno, Poland. Radiocabon 42, 335–348.

Guyodo, Y., Valet, J.-P., 1999. Global changes in intensity of the earth's magnetic field during the past 800 kyr. Nature 399, 249–252.

Halliday, A.N., Lee, D.-C., Christensen, J.N., Walder, A.J., Freedman, P.A., Jones, C.E., Hall, C.M., Yi, W., Teagle, D., 1995. Recent developments in inductively coupled plasma magnetic sector multiple collect mass spectrometry. International Journal of Mass Spectrometry and Ion Processes 146/147, 21–33.

Halliday, A.N., Lee, D.-C., Christensen, J.N., Rehkämper, M., Yi, W., Luo, X., Hall, C.M., Ballentine, C.J., Pettke, T., Stirling, C., 1998. Applications of multiple collector-ICPMS to cosmochemistry, geochemistry and paleoceanography. Geochimica et Cosmochimica Acta 62, 919–940.

Hamelin, B., Bard, E., Zindler, A., Fairbanks, R.G., 1991. $^{234}U/^{238}U$ mass spectrometry of corals: How accurate is the U-Th age of the last interglacial period? Earth and Planetary Science Letters 106, 169–180.

Henderson, G.M., Cohen, A.S., O'Nions, R.K., 1993. $^{234}U/^{238}U$ ratios and ^{230}Th ages for Hateruma Atoll corals: implications for coral diagenesis and seawater $^{234}U/^{238}U$ ratios. Earth and Planetary Science Letters 115, 65–73.

Hughen, K.A., Overpeck, J.T., Lehman, S.J., Kashgarian, M., Southon, J., Peterson, L.C., Alley, R., Sigman, D.M., 1998. Deglacial changes in ocean circulation from an extended radiocarbon calibration. Nature 391, 65–68.

Hughen, K.A., Southon, J.R., Lehman, S.J., Overpeck, J.T., 2000. Synchronous radiocarbon and climate shifts during the last deglaciation. Science 290, 1951–1954.

Hughen, K.A., Lehman, S., Southon, J., Overpeck, J., Marchal, O., Herring, C., Turnbull, J., 2004a. ^{14}C activity and global carbon cycle changes over the past 50,000 years. Science 303 (5655), 202–207.

Hughen, K.A., Baillie, M.G.L., Bard, E., Beck, J.W., Bertand, C.J.H., Blackwell, P.G., Buck, C.E., Burr, G.S., Cutler, K.B., Damon, P.E., Edwards, R.L., Fairbanks, R.G., Friedrich, M., Guilderson, T.P., Kromer, B., McCormac, G., Manning, S., Ramsey, C.B., Reimer, P.J., Reimer, R.W., Remmele, S., Southon, J.R., Stuiver, M., Talamo, S., Taylor, F.W., van der Plicht, J., Weyhenmeyer, C.E., 2004b. Marine04 Marine radiocarbon age calibration, 0–26 ka BP. Radiocarbon 46, 1059–1086.

Johnsen, S.J., Clausen, H.B., Dansgaard, W., Fuhrer, K., Gundestrup, N., Hammer, C.U., Iversen, P., Jouzel, J., Stauffer, B., Steffensen, J.P., 1992. Irregular Glacial Interstadials recorded in a new Greenland ice core. Nature 359, 311–313.

Johnsen, S.J., Dahl-Jensen, D., Dansgaard, W., Gundestrup, N., 1995. Greenland paleotemperatures derived from GRIP bore hole temperature and ice core isotope profiles. Tellus 47 B, 624–629.

Johnsen, S.J., Clausen, H.B., Dansgaard, W., Gundestrup, N.S., Hammer, C.U., Andersen, U., Andersen, K.K., Hvidberg, C.S., Dahl-Jensen, D., Steffensen, J.P., Shoji, H., Sveinbjornsdottir, A.E., White, J., Jouzel, J., Fisher, D., 1997. The delta O-18 record along the Greenland Ice Core Project deep ice core and the problem of possible Eemian climatic instability. Journal of Geophysical Research-Oceans 102, 26397–26410.

Johnsen, S.J., Dahl-Jensen, D., Gundestrup, N., Steffensen, J.P., Clausen, H.B., Miller, H., Masson-Delmotte, V., Sveinbjornsdottir, A.E., White, J., 2001. Oxygen isotope and palaeotemperature records from six Greenland ice-core stations: Camp Century, Dye-3, GRIP, GISP2, Renland and NorthGRIP. Journal of Quaternary Science 16, 299–307.

Kitagawa, H., van der Plicht, J., 2000. Atmospheric radiocarbon calibration beyond 11,900 cal B.P. from Lake Suigetsu laminated sediments. Radiocarbon 42, 369–380.

Kutschera, W., 1999. Accelerator mass spectrometry: analyzing our world atom by atom. American Institute of Physics (AIP) Conference Proceedings 495, 407–428.

Lal, D., 1988. Theoretically expected variations in the terrestrial cosmic-ray production rates of isotope. In: Castagnoli, G.C. (Ed.), Solar-Terrestrial Relationships and the Earth Environment in the Last Millennia. North-Holland, Amsterdam; New York, pp. 216–233.

Lal, D., Peters, B., 1962. Cosmic ray produced isotopes and their application to problems in geophysics. Progress in Elementary Particle and Cosmic Ray Physics 6, 1–74.

Laj, C., Kissel, C., Mazaud, A., Channell, J.E.T., Beer, J., 2000. North Atlantic palaeointensity stack since 75 ka (NAPIS-75) and the duration of the Laschamp event. Philosophical Transactions of the Royal Society of London, Series A, Mathematical Physical and Engineering Sciences 358, 1009–1025.

Laj, C., Kissel, C., Beer, J., 2004. High resolution global paleointensity stack since 75 kyr (GLOPIS-75) calibrated to absolute values. Geophysical Monograph Series 145, 255–265.

Libby, W.F., 1955. Radiocarbon Dating. University of Chicago Press, Chicago 175p.

Luo, X., Rehkämper, M., Lee, D.-C., Halliday, A.N., 1997. High precision $^{230}Th/^{232}Th$ and $^{234}U/^{238}U$ measurements using energy-filtered ICP Magnetic sector multiple collector mass spectrometry. International Journal of Mass Spectrometry and Ion Processes 171, 105–117.

McElhinny, M.W., Senanayake, W.E., 1982. Variations in the geomagnetic dipole 1: The past 50000 years. Journal of Geomagnetism and Geoelectricity 34 (1), 39–51.

Meese, D.A., Gow, A.J., Grootes, P., Mayewski, P.A., Ram, M., Stuiver, M., Taylor, K.C., Waddington, E.D., Zielinski, G.A., 1994. The accumulation record from the GISP2 core as an indicator of climate change throughout the Holocene. Science 266, 1680–1682.

Meese, D.A., Gow, A.J., Alley, R.B., Zielinski, G.A., Grootes, P.M., Ram, M., Taylor, K.C., Mayewski, P.A., Bolzan, J.F., 1997. The Greenland Ice Sheet Project 2 depth-age scale: methods and results. Journal of Geophysical Research, C, Oceans 102 (12), 26411–26423.

Mikolajewicz, U., 1996. A meltwater induced collapse of the 'conveyor belt' thermohaline circulation and its influence on the distribution of $\Delta^{14}O$ and $\delta^{18}O$ in the oceans: Max-Planck-Institut fur Meteortologie Report, no. 189.

Min, G.R., Edwards, R.L., Taylor, F.W., Recy, J., Gallup, C.D., Beck, J.W., 1995. Annual cycles of U/Ca in coral skeletons and U/Ca thermometry. Geochimica et Cosmochimica Acta 59, 2025–2042.

Mortlock, R.A., Fairbanks, R.G., Chiu, T.-C., Rubenstone, J., 2005. $^{230}Th/^{234}U/^{238}U$ and $^{231}Pa/^{235}U$ ages from a single fossil coral fragment by multi-collector magnetic-sector inductively coupled plasma mass spectrometry. Geochimica et Cosmochimica Acta 69 (3), 649–657.

Muscheler, R., Beer, J., Wagner, G., Finkel, R.C., 2000. Changes in deep-water formation during the Younger Dryas event inferred from ^{10}Be and ^{14}C records. Nature 408, 567–570.

Nadeau, M.-J., Schleicher, M., Grootes, P.M., Erlenkeuser, H., Gottdang, A., Mous, D.J.W., Sarnthein, J.M., Willkomm, H., 1997. The Leibniz-Labor AMS facility at the Christian-Albrechts-University, Kiel, Germany. Nuclear Instruments and Methods B in Physics Research Section 123, 22–30.

Nadeau, M.-J., Grootes, P.M., Schleicher, M., Hasselberg, P., Rieck, A., Bitterling, M., 1998. Sample throughput and data quality at the Leibniz-Labor AMS Facility. Radiocarbon 40, 239–245.

Nadeau, M.-J., Grootes, P.M., Voelker, A., Bruhn, F., Duhr, A., Oriwall, A., 2001. Carbonate [14]C Background: Does it have multiple personalities? Radiocarbon 43, 169–176.

Paterne, M., Ayliffe, L.K., Arnold, M., Cabioch, G., Tisnerat-Laborde, N., Hatte, C., Douville, E., Bard, E., 2004. Paired ^{14}C and [230]Th/U dating of surface corals from the Marquesas and Vanuatu (sub-equatorial pacific) in the 3000 to 15,000 Cal yr interval. Radiocarbon 46 (2), 551–566.

Pickett, D.A., Murrell, M.T., Williams, R.W., 1994. Determination of Femtogram Quantities of Protactinium in Geologic Samples by Thermal Ionization Mass Spectrometry. Analytical Chemistry 66, 1044–1049.

Reimer, P.J., Hughen, K.A., Guilderson, T.P., McCormac, G., Baillie, M.G.L., Bard, E., Barratt, P., Beck, J.W., Buck, C.E., Damon, P.E., Friedrich, M., Kromer, B., Ramsey, C.B., Reimer, R.W., Remmele, S., Southon, J.R., Stuiver, M., van der Plicht, J., 2002. Preliminary report of the first workshop of the IntCal04 radiocarbon calibration/comparison working group. Radiocarbon 44 (3), 653–661.

Reimer, P.J., Baillie, M.G.L., Bard, E., Bayliss, A., Beck, J.W., Bertrand, C.J.H., Blackwell, P.G., Buck, C.E., Burr, G.S., Cutler, K.B., Damon, P.E., Edwards, R.L., Fairbanks, R.G., Friedrich, M., Guilderson, T.P., Hogg, A.G., Hughen, K.A., Kromer, B., McCormac, G., Manning, S., Ramsey, C.B., Reimer, R.W., Remmele, S., Southon, J.R., Stuiver, M., Talamo, S., Taylor, F.W., van der Plicht, J., Weyhenmeyer, C.E., 2004. IntCal04 Terrestrial radiocarbon age calibration, 0–26 ka BP. Radiocarbon 46, 1029–1058.

Renne, P.R., Karner, D.B., Ludwig, K.R., 1998. Absolute ages aren't exactly. Science 282, 1840–1841.

Ribaud-Laurenti, A., Hamelin, B., Montaggioni, L., Cardinal, D., 2001. Diagenesis and its impact on Sr/Ca ration in Holocene *Acropora* corals. International Journal of Earth Sciences 90 (2), 438–451.

Schramm, A., Stein, M., Goldstein, S.L., 2000. Calibration of the ^{14}C time scale to >40 ka by [234]U–[230]Th dating of Lake Lisan sediments (last glacial Dead Sea). Earth and Planetary Science Letters 175, 27–40.

Shackleton, N.J., Fairbanks, R.G., Chiu, T.-C., Parrenin, F., 2004. Absolute calibration of the Greenland time scale: implications for Antarctic time scales and for Δ^{14}C. Quaternary Science Reviews 23, 1513–1522.

Southon, J., Roberts, M., 2000. Ten years of sourcery at CAMS/LLNL—evolution of a Cs ion source. Nuclear Instruments and Methods in Physics Research B 172, 257–261.

Spurk, M., Friedrich, M., Hofmann, J., Remmele, S., Frenzel, B., Leuschner, H.H., Kromer, B., 1998. Revisions and extension of the Hohenheim oak and pine chronologies: New evidence about the timing of the Younger Dryas/Preboreal transition. Radiocarbon 40, 1107–1116.

Steier, P., Rom, W., Puchegger, S., 2001. New methods and critical aspects in Bayesian mathematics for ^{14}C calibration. Radiocarbon 43, 373–380.

Stocker, T.F., Wright, D.G., 1996. Rapid changes in ocean circulation and atmospheric radiocarbon. Paleoceanography 11, 773–795.

Stuiver, M., 1961. Variations in radiocarbon concentration and sunspot activity. Journal of Geophysical Research 66, 273–276.

Stuiver, M., 1982. A high-precision calibration of the AD radiocarbon time scale. Radiocarbon 24, 1–26.

Stuiver, M., Polach, H.A., 1977. Discussion: reporting ^{14}C data. Radiocarbon 19, 355–363.

Stuiver, M., Quay, P.D., 1980. Changes in atmospheric carbon-14 attributed to a variable Sun. Science 207, 11–19.

Stuiver, M., Pearson, G.W., 1986. High-precision calibration of the radiocarbon time scale, AD 1950- 500BC. Radiocarbon 28 (2B), 805–838.

Stuiver, M., Kromer, B., Becker, B., Ferguson, C.W., 1986. Radiocarbon age calibration back to 13,300 years BP and the ^{14}C age matching of the German Oak and US bristlecone pine chronologies. Radiocarbon 28 (2B), 969–979.

Stuiver, M., Grootes, P.M., Braziunas, T.F., 1995. The GISP2 δ^{18}O climate record of the past 16,500 years and the role of the Sun, ocean, and volcanoes. Quaternary Research 44, 341–354.

Stuiver, M., Reimer, P.J., Bard, E., Beck, J.W., Burr, G.S., Hughen, K.A., Kromer, B., McCormac, G., van der Plicht, J., Spurk, M., 1998a. INTCAL98 radiocarbon age calibration, 24,000-0 cal BP. Radiocarbon 40, 1041–1083.

Stuiver, M., Reimer, P.J., Braziunas, T.F., 1998b. High-precision radiocarbon age calibration for terrestrial and marine samples. Radiocarbon 40, 1127–1151.

Suess, H.E., 1955. Radiocarbon concentration in modern wood. Science 122, 415–417.

Suess, H.E., 1968. Climatic changes, solar activity, and the cosmic-ray production rate of natural radiocarbon. Meteorological Monographs 8, 146–150.

Suess, H.E., 1970. The three causes of the secular C14 fluctuations, their amplitudes and time constants. In: Radiocarbon variations and absolute chronology, Nobel Symposium. Nobelstiftelsen, Stockholm, International, pp. 595–605.

Taylor, K.C., Hammer, C.U., Alley, R.B., Clausen, H.B., Dahl-Jensen, D., Gow, A.J., Gunderstrup, N.S., Kipfstuhl, J., Moore, J.C., Waddington, E.D., 1993. Electrical conductivity measurements from the GISP2 and GRIP Greenland ice cores. Nature 366, 549–552.

Urmos, J.P., 1985. Oxygen isotopes, sea levels, and uplift of reef terraces, Araki Island, Vanuatu. M.S. dissertation, Cornell University.

van der Plicht, J.W., Beck, J.W., Bard, E., Baillie, M.G.L., Blackwell, P.G., Buck, C.E., Friedrich, M., Guilderson, T.P., Hughen, K.A., Kromer, B., McCormac, F.G., Bronk Ramsey, C., Reimer, O.J., Reimer, R.W., Remmele, S., Richards, D.A., Southon, J.R., Stuiver, M., Weyhenmeyer, C.E., 2004. NOTCAL04-comparison/caliberation ^{14}C records 26–50 cal kyr BP. Radiocarbon 46, 1225–1238.

Voelker, A.H.L., Grootes, P.M., Nadeau, M.-J., Sarntheim, M., 2000. Radiocarbon levels in the Iceland Sea from 25–53 kyr and their link to the earth's magnetic field intensity. Radiocarbon 42, 437–452.

Vogel, J.S., Southon, J.R., Nelson, D.E., 1987. Catalyst and binder effects in the use of filamentous graphite for AMS. Nuclear Instruments and Methods in Physics Research B 29, 50–56.

Vogel, J.C., Kronfeld, J., 1997. Calibration of radiocarbon dates for the late Pleistocene using U/Th dates on stalagmites. Radiocarbon 39, 27–32.

Wahba, G., 1990. Spline Models for Observational Data. Society For Industrial and Applied Mathematic, Philadelphia, PA 169pp.

Walder, A.J., Freedman, P.A., 1992. Isotopic ratio measurement using a double focusing magnetic sector mass analyzer with an inductively coupled plasma as an ion source. Journal of Analytical Atomic Spectrometry 7, 571–575.

Yokoyama, Y., Esat, T.M., Lambeck, K., Fifield, L.K., 2000. Last ice age millennial scale climate changes recorded in Huon Peninsula corals. Radiocarbon 42 (3), 383–401.

Data table for radiocarbon calibration "Version Fairbanks0805"

Sample	Lat.	Long.	Species	U-series I.D.	U (ppm)	1σ	^{232}Th(ppt)	$[^{234}$U/^{238}U] act.	1σ	Initial δ^{234}U	1σ	$[^{230}$Th/^{238}U] act.	$[^{230}$Th/^{234}U] act.	1σ	Cal. age (yr BP)	1σ	^{14}C I.D.	Raw ^{14}C age (yr BP)	Res. corr. ^{14}C age (yr BP)	1σ
BARBADOS	Reservoir age for Barbados data is 365 yr																			
RGF 7-4-2	13.04°N	59.54°W	*P. asteroides*														CAMS 106524	6865	6500	25
RGF 7-4-2				082004LC1	2.6228	0.0007	212	1.1467	0.0005	149.8	1.0	0.0746	0.0651	0.0002	7289	19				
RGF 7-5-5	13.04°N	59.54°W	*A. palmata*														CAMS 106525	8670	8305	25
RGF 7-5-5																	CAMS 106887	8745	8380	35
RGF 7-5-5																	CAMS 106891	8740	8375	40
RGF 7-5-5				082004LC2	2.8279	0.0008	54	1.1446	0.0005	148.5	0.5	0.0944	0.0824	0.0001	9330	17				
RGF 7-9-6	13.04°N	59.54°W	*A. palmata*														CAMS 106526	8325	7960	25
RGF 7-9-6				082004LC3	3.3634	0.0009	404	1.1459	0.0006	149.6	1.0	0.0907	0.0791	0.0002	8936	22				
RGF 7-10-2	13.04°N	59.54°W	*A. palmata*														CAMS 106527	8295	7930	25
RGF 7-10-2																	CAMS 106888	8370	8005	35
RGF 7-10-2				082004LC4	2.8775	0.0007	92	1.1448	0.0006	148.5	1.0	0.0906	0.0791	0.0003	8934	30				
RGF 7-12-2	13.04°N	59.54°W	*A. palmata*														CAMS 106528	8580	8215	25
RGF 7-12-2																	CAMS 106889	8575	8210	35
RGF 7-12-2																	CAMS 106907	8630	8265	30
RGF 7-12-2				082004LC5	3.2067	0.0008	66	1.1455	0.0006	149.4	1.0	0.0928	0.0810	0.0002	9155	18				
RGF 7-16-2	13.04°N	59.54°W	*A. palmata*														CAMS 106529	9005	8640	25
RGF 7-16-2				082104LC1	3.1041	0.0010	49	1.1457	0.0005	149.7	0.5	0.0972	0.0849	0.0002	9618	23				
RGF 7-16-6	13.04°N	59.54°W	*A. palmata*														CAMS 106530	9160	8795	35
RGF 7-16-6				082104LC2	3.0678	0.0009	198	1.1452	0.0005	149.3	1.0	0.1001	0.0874	0.0002	9922	21				
RGF 7-19-3	13.04°N	59.54°W	*A. palmata*														CAMS 106531	9275	8910	30
RGF 7-19-3				082104LC3	2.9900	0.0008	251	1.1446	0.0006	148.8	1.0	0.1003	0.0876	0.0003	9941	33				
RGF 7-19-3																	WHOI OS-5608	9260	8895	55
RGF 7-19-3																	WHOI OS-5646	9310	8945	40
RGF 7-19-3																	WHOI OS-5856	9230	8865	35
RGF 7-26-2	13.04°N	59.54°W	*A. palmata*	112304LC7	2.9829	0.0010	120	1.1415	0.0006	146.0	1.0	0.1080	0.0946	0.0002	10782	22				
RGF 7-26-2				051705LC3	3.0254	0.0007	35	1.1426	0.0005	147.0	0.5	0.1086	0.0950	0.0002	10833	25				
RGF 7-26-2																	WHOI OS-5599	9760	9395	45
RGF 7-26-2																	WHOI OS-5637	9730	9365	40
RGF 7-26-2																	WHOI OS-5847	9680	9315	45
RGF 7-26-2																	CAMS 112215	9680	9315	30
RGF 9-1-2	13.04°N	59.56°W	*M. annularis*	042401KS2	2.2322	0.0006	75	1.1379	0.0004	142.7	0.5	0.1208	0.1062	0.0003	12179	33	CAMS 77013	10610	10245	40
RGF 9-1-2																	CAMS 77026	10540	10175	30
RGF 9-1-6	13.04°N	59.56°W	*M. annularis*	042001DP3	2.4344	0.0005	89	1.1391	0.0004	144.0	0.5	0.1195	0.1049	0.0002	12029	30	CAMS 77008	10600	10235	30
RGF 9-1-7	13.04°N	59.56°W	*M. annularis*	042301JS1	2.4183	0.0009	78	1.1361	0.0005	140.7	0.5	0.1166	0.1027	0.0004	11756	53	CAMS 77018	10590	10225	30
RGF 9-1-7				110101RM1	2.4586	0.0008	61	1.1408	0.0006	145.6	1.0	0.1175	0.1030	0.0002	11791	29				
RGF 9-1-8	13.04°N	59.56°W	*M. annularis*	042301AC2	2.2540	0.0004	60	1.1394	0.0003	144.3	0.5	0.1215	0.1067	0.0007	12239	87	CAMS 77021	10580	10215	30
RGF 9-1-8				050103TC5	2.2631	0.0009	76	1.1369	0.0007	141.7	1.0	0.1208	0.1062	0.0003	12186	42	CAMS 96023	10760	10395	35
RGF 9-2-3	13.04°N	59.56°W	*M. annularis*	042401SG1	2.3840	0.0006	122	1.1373	0.0004	142.1	0.5	0.1192	0.1048	0.0003	12017	32	CAMS 77019	10690	10325	30
RGF 9-2-3				110701RM1	2.3277	0.0006	84	1.1396	0.0005	144.5	0.5	0.1195	0.1048	0.0002	12015	24	CAMS 86523	10715	10350	30
RGF 9-2-5	13.04°N	59.56°W	*M. annularis*	050203LC1	2.2277	0.0005	122	1.1387	0.0005	143.5	0.5	0.1202	0.1055	0.0003	12103	39	CAMS 96024	10850	10485	35
RGF 9-2-5				030405KN1	2.3832	0.0005	187	1.1431	0.0004	148.1	0.5	0.1205	0.1054	0.0003	12091	28	CAMS 96031	10905	10540	35
RGF 9-2-7	13.04°N	59.56°W	*M. annularis*	042001TC1	2.2807	0.0014	105	1.1382	0.0007	143.1	1.0	0.1222	0.1074	0.0004	12327	45	CAMS 77011	10770	10405	30
RGF 9-2-7 rep				110701RM2	2.2254	0.0005	88	1.1389	0.0004	143.8	0.5	0.1220	0.1071	0.0002	12290	28	CAMS 77451	10770	10405	30
RGF 9-3-2	13.04°N	59.56°W	*M. annularis*														CAMS 77015	10760	10395	30
RGF 9-3-2				110501RM1	2.2312	0.0007	95	1.1413	0.0005	146.3	0.5	0.1223	0.1072	0.0001	12303	14	CAMS 82280	10785	10420	25
RGF 9-3-4	13.04°N	59.56°W	*M. annularis*														CAMS 77012	10850	10485	40
RGF 9-3-4				050203LC2	2.4563	0.0007	133	1.1381	0.0006	143.2	1.0	0.1255	0.1103	0.0006	12680	75	CAMS 96025	11030	10665	35
RGF 9-3-6	13.04°N	59.56°W	*A. palmata*	071403LC1	2.7685	0.0007	593	1.1404	0.0004	145.6	0.5	0.1276	0.1119	0.0002	12873	24				
RGF 9-3-6																	CAMS 96026	11395	11030	35
RGF 9-8-2	13.04°N	59.56°W	*A. palmata*	071203TC1	3.1967	0.0007	1124	1.1396	0.0005	145.3	0.5	0.1388	0.1218	0.0002	14100	27	CAMS 96027	12615	12250	40
RGF 9-8-2				112503LC5	3.2283	0.0010	1978	1.1405	0.0005	146.2	1.0	0.1386	0.1215	0.0002	14064	29				

Data table for radiocarbon calibration "Version Fairbanks0805"

Sample	Lat.	Long.	Species	U-series I.D.	U (ppm)	1σ	^{232}Th(ppt)	$[^{234}U/^{238}U]$ act.	1σ	Initial δ^{234}U	1σ	$[^{230}Th/^{238}U]$ act.	$[^{230}Th/^{234}U]$ act.	1σ	Cal. age (yr BP)	1σ	^{14}C I.D.	Raw ^{14}C age (yr BP)	Res. corr. ^{14}C age (yr BP)	1σ
RGF 9-9-7	13.04°N	59.56°W	A. palmata														CAMS 96028	12795	12430	40
RGF 9-9-7				103103LC3	3.0831	0.0010	2923	1.1361	0.0005	141.7	1.0	0.1402	0.1234	0.0002	14295	29				
RGF 9-11-2	13.04°N	59.56°W	A. palmata														CAMS 96029	12735	12370	40
RGF 9-11-2				071103LC3	3.1006	0.0010	43	1.1409	0.0004	146.7	0.5	0.1407	0.1233	0.0002	14283	22				
RGF 9-11-2A				102403TC2	3.2613	0.0011	74	1.1380	0.0005	143.7	1.0	0.1398	0.1228	0.0001	14222	18				
RGF 9-11-2B				102703TCRM5	3.1306	0.0011	53	1.1378	0.0005	143.5	0.5	0.1401	0.1231	0.0002	14259	20				
RGF 9-12-5	13.04°N	59.56°W	A. palmata														CAMS 96030	12735	12370	40
RGF 9-12-5 rep																	CAMS 96032	12825	12460	40
RGF 9-12-5				110103LC2	3.2926	0.0010	1790	1.1369	0.0005	142.6	1.0	0.1413	0.1243	0.0002	14408	20				
RGF 9-12-7A	13.04°N	59.56°W	A. palmata	102403LC3	3.2730	0.0015	137	1.1397	0.0005	145.5	1.0	0.1416	0.1242	0.0001	14394	19				
RGF 9-12-7B				102703LC3	3.3387	0.0010	320	1.1382	0.0005	144.0	0.5	0.1414	0.1242	0.0001	14397	17				
RGF 9-12-7																	CAMS 99002	12730	12365	25
RGF 9-12-7																	CAMS 99011	12830	12465	25
RGF 9-13-3	13.04°N	59.56°W	A. palmata	112503LC6	2.9998	0.0009	46	1.1391	0.0005	144.9	1.0	0.1428	0.1254	0.0002	14539	23				
RGF 9-13-3																	CAMS 99003	12680	12315	30
RGF 9-20-2	13.04°N	59.56°W	A. palmata	082801RM3	3.4946	0.0009	144	1.1368	0.0005	144.0	0.5	0.1748	0.1537	0.0003	18116	37	CAMS 77014	15320	14955	30
RGF 9-20-2																	CAMS 77450	15330	14965	30
RGF 9-20-2																	CAMS 81540	15260	14895	30
RGF 9-20-2																	CAMS 81556	15340	14975	30
RGF 9-20-2																	WHOI OS-5600	15250	14885	55
RGF 9-20-2																	WHOI OS-5638	15300	14935	55
RGF 9-20-2																	WHOI OS-5848	15150	14785	50
RGF 9-21-6	13.04°N	59.56°W	A. palmata														CAMS 81541	15295	14930	30
RGF 9-21-6				081804LC1	3.4312	0.0010	42	1.1350	0.0004	142.2	0.5	0.1750	0.1542	0.0003	18174	33				
RGF 9-21-6																	WHOI OS-5601	15450	15085	80
RGF 9-21-6																	WHOI OS-5639	15450	15085	55
RGF 9-21-6																	WHOI OS-5849	15300	14935	45
RGF 9-21-10	13.04°N	59.56°W	A. palmata	030205JM1	3.3641	0.0009	78	1.1375	0.0006	144.8	1.0	0.1758	0.1545	0.0004	18218	44	CAMS 81542	15400	15035	35
RGF 9-21-11	13.04°N	59.56°W	A. palmata	030205JM1	3.5448	0.0010	76	1.1376	0.0005	144.9	1.0	0.1754	0.1542	0.0005	18176	56	CAMS 81543	15405	15040	30
RGF 9-24-2	13.04°N	59.56°W	A. palmata	081804LC3	3.2501	0.0008	59	1.1360	0.0005	143.4	1.0	0.1799	0.1584	0.0002	18716	28				
RGF 9-24-2																	CAMS 81544	15920	15555	30
RGF 9-24-2																	CAMS 82276	15935	15570	30
RGF 9-24-4	13.04°N	59.56°W	A. palmata	081804LC5	2.9809	0.0010	84	1.1356	0.0005	143.0	1.0	0.1807	0.1591	0.0003	18806	33				
RGF 9-24-4																	CAMS 81545	15830	15465	35
RGF 9-27-5-rep	13.04°N	59.56°W	A. palmata	120902TC1	3.1566	0.0009	74	1.1344	0.0005	141.8	1.0	0.1828	0.1612	0.0004	19075	55	CAMS 86516	16335	15970	45
RGF 9-27-5																	CAMS 81547	16400	16035	35
RGF 9-34-7	13.04°N	59.56°W	P. asteroides	020901RM1	2.8933	0.0007	470	1.1316	0.0005	140.0	0.5	0.2052	0.1813	0.0003	21714	41	CAMS 73923	18550	18185	40
RGF 9-34-7 rep																	CAMS 73952	18550	18185	40
RGF 9-34-8	13.04°N	59.56°W	P. asteroides	121802TC4	2.8490	0.0009	221	1.1362	0.0005	144.8	0.5	0.2068	0.1820	0.0003	21802	41	CAMS 82275	18585	18220	40
RGF 9-34-10	13.04°N	59.56°W	P. asteroides	020901RM2	2.9253	0.0007	205	1.1309	0.0005	139.3	0.5	0.2063	0.1824	0.0003	21858	41	CAMS 73924	18590	18225	40
RGF 9-35-2	13.04°N	59.56°W	P. asteroides	020901RM3	2.9602	0.0008	176	1.1316	0.0005	140.0	0.5	0.2070	0.1829	0.0003	21922	41	CAMS 73925	18670	18305	40
RGF 9-35-2 rep				080201RM3	2.9812	0.0009	189	1.1310	0.0006	139.5	1.0	0.2076	0.1836	0.0003	22010	36	CAMS 73950	18670	18305	40
RGF 9-35-6	13.04°N	59.56°W	M. annularis	020901RM4	2.2615	0.0007	88	1.1325	0.0005	141.1	0.5	0.2092	0.1847	0.0005	22160	62	CAMS 73926	18750	18385	40
RGF9-37-2	13.04°N	59.56°W	M. annularis	121902TC1	2.1611	0.0006	93	1.1317	0.0005	140.4	0.5	0.2122	0.1875	0.0003	22536	46	CAMS 86507	19450	19085	60
RGF9-37-2rep																	CAMS 86517	19470	19105	60
RGF 9-37-3	13.04°N	59.56°W	M. annularis	021201RM2	2.1890	0.0006	91	1.1317	0.0004	140.4	0.5	0.2125	0.1878	0.0004	22574	48	CAMS 73927	19360	18995	40
RGF 9-38-1	13.04°N	59.56°W	M. annularis	121100RM4	2.3490	0.0007	73	1.1315	0.0005	140.4	1.0	0.2165	0.1913	0.0003	23044	37	CAMS 73928	19820	19455	40
RGF 9-38-2	13.04°N	59.56°W	M. annularis	102400RM1	2.3305	0.0008	96	1.1292	0.0006	138.0	1.0	0.2182	0.1932	0.0005	23296	61	CAMS 73929	19720	19355	40

Data table for radiocarbon calibration "Version Fairbanks0805"

Sample	Lat.	Long.	Species	U-series I.D.	U (ppm)	1 σ	232Th(ppt)	[234U/238U] act.	1 σ	Initial δ234U	1 σ	[230Th/238U] act.	[230Th/234U] act.	1 σ	Cal. age (yr BP)	1 σ	14C I.D.	Raw 14C age (yr BP)	Res. corr. 14C age (yr BP)	1σ
RGF 9-38-3	13.04°N	59.56°W	*M. annularis*	102400RM2	2.3162	0.0011	76	1.1293	0.0007	138.0	1.0	0.2160	0.1913	0.0003	23039	38	CAMS 73930	19750	19385	40
RGF 9-39-2	13.04°N	59.56°W	*M. annularis*	102400RM3	2.5734	0.0007	98	1.1289	0.0005	137.9	0.5	0.2229	0.1974	0.0003	23867	44	CAMS 73931	20310	19945	50
RGF 9-39-3	13.04°N	59.56°W	*M. annularis*	102500RM1	2.4016	0.0029	140	1.1307	0.0011	139.9	1.5	0.2232	0.1974	0.0005	23858	69	CAMS 73932	20260	19895	40
RGF 9-39-4	13.04°N	59.56°W	*Diploria*	102500RM2	2.5005	0.0006	113	1.1287	0.0006	138.1	1.0	0.2313	0.2049	0.0004	24883	55	CAMS 73933	21080	20715	40
RGF 9-39-5	13.04°N	59.56°W	*Diploria*														CAMS 73934	21100	20735	50
RGF 9-39-5				102600RM1	2.2382	0.0005	1296	1.1302	0.0004	139.5	0.5	0.2291	0.2027	0.0003	24579	41	CAMS 73935	20930	20565	50
RGF 9-39-5 rep																	CAMS 73947	20990	20625	50
RGF 9-39-5				112304LC5	2.6860	0.0008	202	1.1298	0.0005	139.1	1.0	0.2287	0.2024	0.0002	24549	31	CAMS 81548	21040	20675	45
RGF 9-39-5																	WHOI OS-5621	21100	20735	90
RGF 9-39-5																	WHOI OS-5659	21300	20935	130
RGF 9-39-5																	WHOI OS-5869	21000	20635	100
RGF 9-41-3	13.04°N	59.56°W	*M. annularis*	102600RM2	2.3011	0.0005	166	1.1293	0.0005	139.0	1.0	0.2378	0.2105	0.0003	25645	40	CAMS 73938	21670	21305	50
RGF 9-41-6	13.04°N	59.56°W	*M. annularis*														CAMS 73939	21760	21395	50
RGF 9-41-6				110101RM2	2.1185	0.0006	76	1.1281	0.0005	137.8	1.0	0.2383	0.2112	0.0004	25743	61				
RGF 9-41-6																	WHOI OS-5609	21800	21435	85
RGF 9-41-6																	WHOI OS-5857	21700	21335	90
RGF 9-41-6																	WHOI OS-5857	21900	21535	75
RGF9-41-8	13.04°N	59.56°W	*M. annularis*	011601RM3	2.1469	0.0004	58	1.1287	0.0004	138.4	0.5	0.2376	0.2105	0.0003	25639	45	CAMS 73940	21680	21315	50
RGF 9-41-8 rep																	CAMS 73948	21720	21355	50
RGF 9-41-8 rep																	CAMS 76153	21820	21455	50
RGF 9-41-9	13.04°N	59.56°W	*M. annularis*	011701RM1	2.4180	0.0005	68	1.1299	0.0004	139.7	0.5	0.2387	0.2112	0.0004	25741	53	CAMS 73941	21760	21395	50
RGF 9-41-10	13.04°N	59.56°W	*M. annularis*	011701RM2	2.2724	0.0006	78	1.1300	0.0006	139.9	1.0	0.2397	0.2121	0.0004	25866	53	CAMS 73942	21790	21425	50
RGF 9-41-13	13.04°N	59.56°W	*M. annularis*	011701RM3	2.2514	0.0006	164	1.1285	0.0004	138.4	0.5	0.2428	0.2151	0.0004	26278	50	CAMS 73944	22070	21705	50
RGF 9-41-13				080801RM1	2.3937	0.0006	281	1.1283	0.0005	138.1	0.5	0.2408	0.2134	0.0003	26044	40				
RGF 12-5-2	13.05°N	59.55°W	*A. palmata*														CAMS 99004	10270	9905	25
RGF 12-5-2A				102803RMTC1	3.5148	0.0014	596	1.1407	0.0006	145.4	1.0	0.1137	0.0997	0.0002	11393	30				
RGF 12-5-2B				102703LC4	3.5533	0.0013	382	1.1411	0.0005	145.8	0.5	0.1137	0.0997	0.0001	11390	14				
RGF 12-9-3	13.05°N	59.55°W	*A. palmata*	050103TC1	2.6846	0.0009	266	1.1364	0.0005	141.1	1.0	0.1190	0.1047	0.0002	12002	25				
RGF 12-9-3																	CAMS 99005	10540	10175	25
RGF 12-9-5	13.05°N	59.55°W	*A. palmata*	050103TC3	2.7979	0.0007	349	1.1383	0.0005	143.1	0.5	0.1211	0.1064	0.0003	12203	38				
RGF 12-9-5																	CAMS 99006	10485	10120	35
RGF 12-9-6	13.05°N	59.55°W	*A. palmata*														CAMS 99007	10505	10140	25
RGF 12-9-6				110103LC4	3.2726	0.0012	1726	1.1387	0.0005	143.5	0.5	0.1208	0.1061	0.0001	12170	15				
RGF 12-14-2	13.05°N	59.55°W	*A. palmata*	081904LC1	3.0456	0.0011	652	1.1399	0.0006	145.1	1.0	0.1286	0.1129	0.0003	12996	30				
RGF 12-14-2				030205LB2	3.3008	0.0009	582	1.1405	0.0006	145.7	1.0	0.1270	0.1114	0.0003	12816	37	CAMS 99009	11265	10900	25
RGF 12-15-4	13.05°N	59.55°W	*A. palmata*														CAMS 99625	11405	11040	25
RGF 12-15-4				103003RM1	3.1464	0.0008	153	1.1384	0.0005	143.7	1.0	0.1291	0.1134	0.0001	13066	17				
RGF 12-15-4				110303LC2	3.1412	0.0010	127	1.1397	0.0005	145.0	0.5	0.1279	0.1122	0.0001	12919	17				
RGF 12-15-4																	WHOI OS-5604	11500	11135	45
RGF 12-15-4																	WHOI OS-5642	11400	11035	45
RGF 12-15-4																	WHOI OS-5852	11550	11185	40
RGF 12-21-2	13.05°N	59.55°W	*A. palmata*														CAMS 99627	11925	11560	30
RGF 12-21-2 rep																	CAMS 99631	11880	11515	25
RGF 12-21-2				103103LC1	3.0404	0.0008	184	1.1374	0.0006	142.8	1.0	0.1335	0.1174	0.0002	13555	19				
RGF 12-21-6	13.05°N	59.55°W	*A. palmata*														CAMS 99628	11945	11580	35
RGF 12-21-6				110303LC3	3.0205	0.0011	107	1.1374	0.0005	142.8	0.5	0.1337	0.1176	0.0002	13574	26				
RGF 12-21-7	13.05°N	59.55°W	*A. palmata*	112603LC2	2.8969	0.0010	65	1.1386	0.0007	144.1	1.0	0.1339	0.1176	0.0002	13578	26				
RGF 12-21-7																	CAMS 99629	11935	11570	30
RGF 12-21-7																	WHOI OS-5606	11900	11535	40
RGF 12-21-7																	WHOI OS-5644	11850	11485	65
RGF 12-21-7																	WHOI OS-5854	11950	11585	40

Data table for radiocarbon calibration "Version Fairbanks0805"

Sample	Lat.	Long.	Species	U-series I.D.	U (ppm)	1 σ	²³²Th(ppt)	[²³⁴U/²³⁸U] act.	1 σ	Initial δ²³⁴U	1 σ	[²³⁰Th/²³⁸U] act.	[²³⁰Th/²³⁴U] act.	1 σ	Cal. age (yr BP)	1 σ	¹⁴C I.D.	Raw ¹⁴C age (yr BP)	Res. corr. ¹⁴C age (yr BP)	1σ
RGF 12-21-10	13.05°N	59.55°W	*A. palmata*														CAMS 99630	12075	11710	30
RGF 12-21-10				110303LC5	3.4760	0.0010	186	1.1385	0.0005	144.0	1.0	0.1344	0.1180	0.0001	13632	16				
RGF 12-28-6	13.05°N	59.55°W	*A. palmata*	121801TC1	3.1239	0.0008	365	1.1298	0.0005	141.1	0.7	0.2698	0.2388	0.0003	29590	44	CAMS 73919	25290	24925	60
RGF 12-28-6 rep																	CAMS 73953	25340	24975	70
RGF 12-28-7	13.05°N	59.55°W	*A. palmata*	021301RM2	2.9820	0.0005	482	1.1274	0.0004	138.7	0.5	0.2742	0.2432	0.0004	30214	56	CAMS 73920	25320	24955	60
RGF 12-28-7 rep				073101RM2	3.2159	0.0008	863	1.1284	0.0005	139.9	0.5	0.2734	0.2423	0.0004	30080	58	CAMS 73949	25180	24815	60
RGF 12-28-7 rep																	CAMS 75385	25210	24845	90
RGF 12-28-7 rep																	CAMS 77432	25280	24915	90
RGF 12-29-2	13.05°N	59.55°W	*A. palmata*	080201RM2	3.2406	0.0007	68	1.1269	0.0004	138.3	0.5	0.2742	0.2433	0.0003	30225	40	CAMS 73921	25320	24955	70
RGF 12-29-2 rep																	CAMS 73946	25280	24915	70
RGF 13-1-11	13.04°N	59.55°W	*A. palmata*	112603LC3	2.5466	0.0011	54	1.1377	0.0007	143.5	1.0	0.1432	0.1258	0.0002	14596	26				
RGF 13-1-11																	WHOI OS-5610	12950	12585	60
RGF 13-1-11																	WHOI OS-5648	12800	12435	70
RGF 13-1-11																	WHOI OS-5858	12800	12435	40
RGF 13-8-9	13.04°N	59.55°W	*A. palmata*	082801RM2	3.3690	0.0010	120	1.1322	0.0004	138.9	0.5	0.1693	0.1495	0.0005	17580	69				
RGF 13-8-9																	CAMS 81539	14785	14420	30
RGF 13-8-9rep																	CAMS 88790	14915	14550	35
RGF 15-2-4	13.04°N	59.55°W	*M. annularis*	082001RM1	2.2687	0.0004	60	1.1393	0.0004	144.4	0.5	0.1243	0.1091	0.0002	12533	26	CAMS 81550	10885	10520	25
RGF 15-2-4																	CAMS 82278	10800	10435	25
RGF 15-2-4																	WHOI OS-5614	10900	10535	50
RGF 15-2-4																	WHOI OS-5652	10950	10585	45
RGF 15-2-4																	WHOI OS-5862	10950	10585	35
RGF 15-4-1	13.04°N	59.55°W	*M. annularis*	081904LC2	2.2243	0.0008	124	1.1397	0.0006	145.0	1.0	0.1280	0.1123	0.0004	12926	49	CAMS 81551	11020	10655	25
RGF 15-4-1				030405ZA2	2.3647	0.0005	299	1.1419	0.0006	147.1	1.0	0.1275	0.1116	0.0003	12844	29	CAMS 82279	11045	10680	25
RGF 15-5-1	13.04°N	59.55°W	*M. annularis*														CAMS 81552	11465	11100	35
RGF 15-5-1				112603LC4	2.6421	0.0009	30	1.1413	0.0005	146.6	1.0	0.1278	0.1119	0.0002	12883	19				
RGF 15-5-1				081904LC3	2.4090	0.0010	18	1.1405	0.0006	145.7	1.0	0.1279	0.1121	0.0004	12907	54				
RGF 15-5-2	13.04°N	59.55°W	*M. annularis*														CAMS 82283	11505	11140	25
RGF 15-5-2				112603LC5	2.4671	0.0008	25	1.1410	0.0006	146.3	1.0	0.1289	0.1130	0.0002	13013	23				
RGF 15-5-3	13.04°N	59.55°W	*A. palmata*														CAMS 81553	12730	12365	35
RGF 15-5-3				110103LC3	3.0026	0.0008	48	1.1385	0.0005	144.4	1.0	0.1431	0.1256	0.0001	14573	15				
RGF 15-7-1	13.04°N	59.55°W	*M. annularis*														CAMS 81554	12880	12515	25
RGF 15-7-1				011305LC1	2.5444	0.0006	69	1.1420	0.0006	148.0	1.0	0.1445	0.1266	0.0002	14685	22	CAMS 82284	12880	12515	30
RGF 15-8-1	13.04°N	59.55°W	*A. palmata*	110501RM2	3.2461	0.0008	232	1.1328	0.0005	140.0	0.5	0.1775	0.1567	0.0003	18494	36	CAMS 81555	15290	14925	35
RGF 15-8-1																	CAMS 82285	15315	14950	25
RGF15-9-5	13.04°N	59.55°W	*A. palmata*	121702TC3	2.9631	0.0008	50	1.1367	0.0004	144.0	0.5	0.1773	0.1560	0.0002	18408	26	CAMS 86508	15200	14835	40
RGF15-9-5rep																	CAMS 86518	15175	14810	40
RGF 15-10-1	13.04°N	59.55°W	*A. palmata*	110601RM2	2.9765	0.0006	111	1.1320	0.0004	139.5	0.5	0.1856	0.1640	0.0002	19438	25	CAMS 88770	16155	15790	40
RGF 15-10-1				011305LC2	3.0816	0.0010	87	1.1385	0.0005	146.3	0.5	0.1859	0.1633	0.0004	19345	53	CAMS 88784	16165	15800	40
RGF 15-10-2	13.04°N	59.55°W	*A. palmata*	012405LC3	3.1666	0.0011	80	1.1367	0.0006	144.4	1.0	0.1865	0.1641	0.0003	19450	36	CAMS 88771	16470	16105	35
RGF 15-10-2																	CAMS 88792	16490	16125	40
RGF 15-10-3	13.04°N	59.55°W	*A. palmata*	012805LC3	3.4969	0.0010	128	1.1378	0.0005	145.5	0.5	0.1845	0.1622	0.0003	19203	37	CAMS 88772	16170	15805	40
RGF 15-10-3																	CAMS 88785	16200	15835	40
RGF 15-10-3																	CAMS 99010	16225	15860	40
RGF 15-10-4	13.04°N	59.55°W	*A. palmata*	012805LC4	3.3298	0.0009	115	1.1395	0.0005	147.1	0.5	0.1796	0.1576	0.0002	18617	21				
RGF 15-10-4																	CAMS 88773	15765	15400	35
RGF15-10-5	13.04°N	59.55°W	*A. palmata*	121702TC2	3.2326	0.0006	69	1.1369	0.0004	144.1	0.5	0.1732	0.1523	0.0002	17935	26	CAMS 86509	15090	14725	45
RGF 15-10-5 rep																	CAMS 99025	15020	14655	30
RGF 15-10-6	13.04°N	59.55°W	*A. palmata*	082001RM2	3.2205	0.0007	73	1.1339	0.0004	140.9	0.5	0.1732	0.1528	0.0003	17996	35				
RGF 15-10-6																	CAMS 86520	15015	14650	40

Data table for radiocarbon calibration "Version Fairbanks0805"

Sample	Lat.	Long.	Species	U-series I.D.	U (ppm)	1σ	^{232}Th(ppt)	$[^{234}$U/^{238}U] act.	1σ	Initial δ^{234}U	1σ	$[^{230}$Th/^{238}U] act.	$[^{230}$Th/^{234}U] act.	1σ	Cal. age (yr BP)	1σ	^{14}C I.D.	Raw ^{14}C age (yr BP)	Res. corr. ^{14}C age (yr BP)	1σ
RGF 15-12-2	13.04°N	59.55°W	*A. palmata*	082101RM1	3.1079	0.0010	151	1.1321	0.0006	139.6	1.0	0.1869	0.1651	0.0002	19581	26	CAMS 86521	16475	16110	45
RGF 15-12-2				033005PS2	3.2964	0.0007	75	1.1356	0.0005	143.3	0.5	0.1864	0.1641	0.0003	19455	40				
RGF 15-12-4	13.04°N	59.55°W	*A. palmata*	082101RM2	3.2327	0.0010	139	1.1311	0.0004	138.5	0.5	0.1846	0.1632	0.0002	19337	23	CAMS 88774	16465	16100	40
RGF 15-13-4	13.04°N	59.55°W	*M. annularis*	082101RM4	2.1758	0.0005	620	1.1334	0.0004	141.0	0.5	0.1887	0.1665	0.0003	19770	32				
RGF 15-13-4				013105LC1	2.2050	0.0006	74	1.1367	0.0006	144.5	1.0	0.1886	0.1659	0.0003	19684	39	CAMS 86510	16745	16380	45
RGF 15-13-4																	CAMS 86519	16725	16360	50
RGF 15-13-6	13.04°N	59.55°W	*Diploria sp*	082201RM1	2.8231	0.0007	551	1.1319	0.0004	139.4	0.5	0.1856	0.1639	0.0002	19434	30	CAMS 88776	16855	16490	40
RGF 15-13-6rep																	CAMS 88786	16835	16470	40
RGF 15-14-3	13.04°N	59.55°W	*M. annularis*	082201RM2	2.4806	0.0005	69	1.1325	0.0004	140.0	0.5	0.1861	0.1643	0.0002	19483	27	CAMS 86511	16975	16610	45
RGF 15-14-4	13.04°N	59.55°W	*M. annularis*	082201RM3	2.3337	0.0010	71	1.1334	0.0005	141.0	1.0	0.1876	0.1655	0.0002	19638	25	CAMS 88777	16980	16615	35
RGF 15-14-4rep																	CAMS 88787	16885	16520	40
RGF 15-14-4																	WHOI OS-5616	17000	16635	85
RGF 15-14-4																	WHOI OS-5654	17000	16635	75
RGF 15-14-4																	WHOI OS-5864	16850	16485	55
RGF 15-14-5	13.04°N	59.55°W	*M. annularis*	022805JD2	2.4657	0.0006	591	1.1367	0.0006	144.4	1.0	0.1864	0.1640	0.0003	19443	30	CAMS 88778	16985	16620	35
RGF 15-14-7	13.04°N	59.55°W	*Diploria sp*	050131LC2	2.4323	0.0011	88	1.1375	0.0007	145.3	1.0	0.1886	0.1658	0.0003	19678	33				
RGF 15-14-7																	CAMS 88779	16950	16585	45
RGF 15-15-2	13.04°N	59.55°W	*Diploria sp*														CAMS 86512	17065	16700	50
RGF 15-15-2rep																	CAMS 86522	17080	16715	45
RGF 15-15-2				040502RM1	2.3962	0.0005	114	1.1356	0.0004	143.4	0.5	0.1883	0.1658	0.0005	19677	64				
RGF 15-15-3	13.04°N	59.55°W	*Diploria sp*	040502RM2	2.6847	0.0006	322	1.1353	0.0006	143.1	1.0	0.1875	0.1652	0.0003	19595	44	CAMS 88780	17025	16660	40
RGF 15-15-3rep																	CAMS 88793	17115	16750	40
RGF 15-15-5	13.04°N	59.55°W	*Diploria sp*	121702TC1	2.5048	0.0006	272	1.1354	0.0005	143.1	0.5	0.1878	0.1654	0.0003	19627	34	CAMS 86513	17150	16785	45
RGF 15-15-7	13.04°N	59.55°W	*M. annularis*	050131LC3	2.3250	0.0006	106	1.1367	0.0006	144.7	1.0	0.1921	0.1690	0.0003	20085	34				
RGF 15-15-7																	CAMS 88781	17125	16760	40
RGF 15-15-8	13.04°N	59.55°W	*M. annularis*	110101RM3	2.3303	0.0005	57	1.1310	0.0004	138.6	0.5	0.1896	0.1676	0.0003	19913	34	CAMS 88782	17220	16855	40
RGF 15-15-8rep																	CAMS 88788	17215	16850	40
RGF 15-15-8																	WHOI OS-5617	17250	16885	75
RGF 15-15-8																	WHOI OS-5655	17200	16835	60
RGF 15-15-8																	WHOI OS-5865	17150	16785	50
RGF 15-15-9	13.04°N	59.55°W	*M. annularis*	013105LC4	2.4147	0.0008	56	1.1364	0.0006	144.4	1.0	0.1920	0.1689	0.0002	20082	27	CAMS 88783	17175	16810	40
RGF 15-15-9																	CAMS 88789	17230	16865	40
RGF 15-17-2	13.04°N	59.55°W	*M. annularis*	012405LC2	2.4942	0.0009	296	1.1387	0.0005	147.0	0.5	0.1972	0.1732	0.0003	20634	39				
RGF 15-17-2																	KIA 25004	17745	17380	60
RGF 15-17-3	13.04°N	59.55°W	*M. annularis*	110103LC5	2.4143	0.0005	60	1.1318	0.0004	139.7	0.5	0.1954	0.1727	0.0002	20575	31	KIA 25003	17825	17460	55
RGF 15-18-1	13.04°N	59.55°W	*M. annularis*	011305LC7	2.3289	0.0004	47	1.1359	0.0005	144.1	0.5	0.1953	0.1719	0.0003	20469	32				
RGF 15-18-1																	KIA 25002	17670	17305	50
RGF 15-18-2	13.04°N	59.55°W	*M. annularis*	011705RM1	2.4614	0.0008	112	1.1382	0.0006	146.5	1.0	0.1969	0.1730	0.0007	20614	90				
RGF 15-18-2																	KIA 25001	17800	17435	55
RGF 15-18-3	13.04°N	59.55°W	*M. annularis*	013105LC5	2.2454	0.0007	60	1.1358	0.0006	144.0	1.0	0.1975	0.1739	0.0003	20734	31				
RGF 15-18-3																	KIA 25000	17740	17375	70
RGF 15-18-4	13.04°N	59.55°W	*M. annularis*	013105LC6	2.4503	0.0008	37	1.1356	0.0005	143.8	0.5	0.1973	0.1738	0.0004	20714	43				
RGF 15-18-4																	KIA 24999	17860	17495	60
RGF 15-19-2	13.04°N	59.55°W	*M. annularis*	030405SS5	2.4718	0.0007	76	1.1341	0.0007	142.1	1.0	0.1952	0.1772	0.0003	20504	39	KIA 24998	17980	17615	60
RGF 15-19-3	13.04°N	59.55°W	*M. annularis*	110303LC1	2.5505	0.0009	65	1.1314	0.0005	139.3	1.0	0.1959	0.1731	0.0002	20632	31				
RGF 15-19-3																	KIA 24997	18110	17745	60
RGF 16-12-6	13.05°N	59.55°W	*A. palmata*	082801RM1	2.9905	0.0008	75	1.1374	0.0004	141.9	0.5	0.1145	0.1007	0.0001	11512	17	CAMS 86514	10335	9970	30

Data table for radiocarbon calibration "Version Fairbanks0805"

Sample	Lat.	Long.	Species	U-series I.D.	U (ppm)	1σ	^{232}Th(ppt)	$[^{234}$U/^{238}U] act.	1σ	Initial δ^{234}U	1σ	$[^{230}$Th/^{238}U] act.	$[^{230}$Th/^{234}U] act.	1σ	Cal. age (yr BP)	1σ	^{14}C I.D.	Raw ^{14}C age (yr BP)	Res. corr. ^{14}C age (yr BP)	1σ
KIRITIMATI	Reservoir age for Kiritimati data is 350 yr																			
CHR 4-1-7	1.99°N	157.78°W	A. hyacinthus	110299RM6	3.6293	0.0010	41	1.1404	0.0005	145.2	1.0	0.1181	0.1035	0.0001	11859	26	CAMS77428	10540	10190	30
CHR 4-2-4	1.99°N	157.78°W	A. hyacinthus	110399RM1	3.5372	0.0010	31	1.1404	0.0005	145.4	1.0	0.1237	0.1085	0.0001	12461	23	CAMS75379	10730	10380	30
CHR 4-2-4																	CAMS75383	10680	10330	30
CHR 4-2-7	1.99°N	157.78°W	A. hyacinthus	070803RM1	3.8200	0.0010	24	1.1439	0.0005	149.2	1.0	0.1265	0.1106	0.0002	12716	28	CAMS75372	11280	10930	30
CHR 4-2-9	1.99°N	157.78°W	A. hyacinthus	070803RM2	3.9030	0.0010	14	1.1413	0.0005	146.5	1.0	0.1273	0.1116	0.0002	12836	25	CAMS75376	11290	10940	30
CHR 4-3-1A	1.99°N	157.78°W	A. hyacinthus	070803RM3	4.0809	0.0010	46	1.1421	0.0005	147.4	1.0	0.1286	0.1126	0.0002	12961	30	CAMS77020	11440	11090	30
CHR 4-3-2	1.99°N	157.78°W	A. hyacinthus	070903RM1	3.6565	0.0010	32	1.1414	0.0005	146.7	1.0	0.1285	0.1126	0.0002	12959	21	CAMS75378	11420	11070	30
CHR 4-3-3	1.99°N	157.78°W	A. hyacinthus	070903RM2	3.8861	0.0010	41	1.1426	0.0005	147.9	1.0	0.1289	0.1128	0.0002	12990	28	CAMS75368	11410	11060	30
CHR 4-3-8	1.99°N	157.78°W	A. hyacinthus	070903RM3	3.0028	0.0010	48	1.1414	0.0006	146.8	1.0	0.1300	0.1139	0.0002	13117	29	CAMS77439	11660	11310	30
CHR 4-3-15	1.99°N	157.78°W	A. hyacinthus	101899RM1	2.8057	0.0010	42	1.1391	0.0005	144.6	1.0	0.1346	0.1182	0.0002	13650	45	CAMS77016	11930	11580	30
CHR 4-3-15			A. hyacinthus	071003RM1	2.5690	0.0010	200	1.1397	0.0006	145.2	1.0	0.1351	0.1186	0.0003	13698	41				
CHR 5-1-3	1.99°N	157.78°W	A. hyacinthus	120399RM3	3.7147	0.0010	80	1.1406	0.0005	145.3	1.0	0.1150	0.1008	0.0001	11527	25	CAMS75370	10260	9910	30
CHR 5-1-5	1.99°N	157.78°W	A. hyacinthus	040202RM2	3.2960	0.0010	14	1.1426	0.0004	147.4	1.0	0.1154	0.1010	0.0001	11548	21	CAMS75366	10360	10010	30
CHR 5-1-5																	CAMS75381	10350	10000	30
CHR 5-1-8	1.99°N	157.78°W	A. hyacinthus	030200RM1	3.7659	0.0010	46	1.1421	0.0005	146.9	1.0	0.1177	0.1031	0.0002	11805	38	CAMS77445	10480	10130	30
CHR 5-1-9	1.99°N	157.78°W	A. hyacinthus	040202RM3	3.8240	0.0010	28	1.1398	0.0004	144.6	1.0	0.1188	0.1043	0.0002	11949	21	CAMS75374	10550	10200	30
CHR 5-1-11A	1.99°N	157.78°W	A. hyacinthus	080101RM1	4.0324	0.0010	69	1.1395	0.0004	144.3	1.0	0.1186	0.1041	0.0001	11925	12	CAMS75367	10560	10210	30
CHR 5-2-2	1.99°N	157.78°W	A. hyacinthus	040302RM1	3.1310	0.0010	8	1.4060	0.0004	145.3	1.0	0.1156	0.1013	0.0001	11591	15	CAMS75375	10310	9960	40
CHR 5-2-3	1.99°N	157.78°W	A. hyacinthus	040302RM2	3.5050	0.0010	11	1.4070	0.0003	145.6	1.0	0.1188	0.1041	0.0001	11931	18	CAMS77442	10500	10150	30
CHR 5-2-4	1.99°N	157.78°W	A. hyacinthus	040302RM3	3.5860	0.0010	25	1.1396	0.0004	144.4	1.0	0.1193	0.1047	0.0002	11996	26	CAMS75373	10580	10230	40
CHR 5-2-4																	CAMS75382	10480	10130	30
CHR 6-1-2	1.99°N	157.78°W	A. hyacinthus	060499RM3	3.5180	0.0010	58	1.1407	0.0004	145.4	1.0	0.1154	0.1012	0.0001	11571	24	CAMS76145	10390	10040	30
CHR 6-1-2			A. hyacinthus	063099RM5	3.5100	0.0010	61	1.1385	0.0005	143.2	1.0	0.1163	0.1022	0.0002	11697	25	CAMS76155	10390	10040	40
CHR 6-1-3	1.99°N	157.78°W	A. hyacinthus	060899RM2	3.0925	0.0010	46	1.1423	0.0004	147.1	1.0	0.1155	0.1011	0.0001	11569	28	CAMS77438	10360	10010	30
CHR 6-1-3			A. hyacinthus	063099RM4	3.0830	0.0010	47	1.1437	0.0004	148.5	1.0	0.1161	0.1015	0.0001	11612	22				
CHR 6-2-2	1.99°N	157.78°W	A. hyacinthus	060799RM2	3.5480	0.0010	22	1.1412	0.0004	146.1	1.0	0.1180	0.1034	0.0001	11839	22	CAMS77024	11590	10240	30
CHR 6-2-2			A. hyacinthus	063099RM4	3.5500	0.0010	22	1.1376	0.0004	142.3	1.0	0.1183	0.1040	0.0001	11920	23				
CHR 6-2-5	1.99°N	157.78°W	A. hyacinthus	060899RM4	3.6531	0.0010	65	1.1397	0.0004	144.6	1.0	0.1209	0.1061	0.0001	12172	30	CAMS77441	10710	10360	30
CHR 6-2-5			A. hyacinthus	060301RM1	3.6564	0.0010	56	1.1408	0.0006	145.7	1.0	0.1204	0.1055	0.0001	12103	16				
CHR 6-2-6	1.99°N	157.78°W	A. hyacinthus	060899RM4	3.7551	0.0010	58	1.1399	0.0004	144.8	1.0	0.1220	0.1071	0.0001	12287	29	CAMS76150	10770	10420	30
CHR 6-2-6			A. hyacinthus	063099RM6	3.7447	0.0010	61	1.1397	0.0004	144.7	1.0	0.1222	0.1072	0.0001	12304	23				
CHR 6-2-7	1.99°N	157.78°W	A. hyacinthus	030100RM2	3.6195	0.0010	43	1.1397	0.0004	144.8	1.0	0.1242	0.1090	0.0002	12526	40	CAMS77433	10730	10380	30
CHR 6-2-8	1.99°N	157.78°W	A. hyacinthus	030300RM1	3.8582	0.0010	114	1.1375	0.0004	142.5	1.0	0.1242	0.1092	0.0002	12553	47	CAMS77443	10850	10500	30
CHR 6-2-10	1.99°N	157.78°W	A. hyacinthus	101599RM1	3.9214	0.0010	61	1.1406	0.0004	145.8	1.0	0.1251	0.1097	0.0002	12611	38	CAMS77430	10900	10550	30
CHR 7-1-2	1.99°N	157.78°W	unidentified sp.	080101RM1	3.0000	0.0010	84	1.1409	0.0005	145.2	1.0	0.1063	0.0932	0.0001	10612	17	CAMS76146	9730	9380	30
CHR 7-1-4	1.99°N	157.78°W	unidentified sp.	080301RM2	2.8325	0.0010	124	1.1391	0.0006	143.4	1.0	0.1062	0.0932	0.0001	10615	26	CAMS76144	9800	9450	30
CHR 7-1-5	1.99°N	157.78°W	unidentified sp.	080301RM3	2.7688	0.0010	64	1.1407	0.0005	145.0	1.0	0.1066	0.0934	0.0001	10642	19	CAMS76141	9700	9350	30
CHR 7-1-7	1.99°N	157.78°W	A. hyacinthus	070299RM1	3.4695	0.0010	59	1.1387	0.0004	143.4	1.0	0.1157	0.1016	0.0001	11625	23	CAMS76139	10440	10090	30
CHR 7-1-7																	CAMS76158	10380	10030	40

Data table for radiocarbon calibration "Version Fairbanks0805"

Sample	Lat.	Long.	Species	U-series I.D.	U (ppm)	1 σ	^{232}Th(ppt)	$[^{234}$U/^{238}U] act.	1 σ	Initial δ^{234}U	1 σ	$[^{230}$Th/^{238}U] act.	$[^{230}$Th/^{234}U] act.	1 σ	Cal. age (yr BP)	1 σ	^{14}C I.D.	Raw ^{14}C age (yr BP)	Res. corr. ^{14}C age (yr BP)	1σ
CHR 7-2-2	1.99°N	157.78°W	*A. hyacinthus*	071999RM8	3.5889	0.0010	65	1.1377	0.0003	142.6	1.0	0.1199	0.1054	0.0002	12081	42	CAMS77436	10590	10240	30
CHR 7-2-2																	CAMS77448	10580	10230	30
CHR 7-2-6	1.99°N	157.78°W	*A. hyacinthus*	030300RM2	3.4285	0.0010	24	1.1384	0.0003	143.2	1.0	0.1210	0.1063	0.0002	12199	41	CAMS77025	10620	10270	30
CHR 7-2-8	1.99°N	157.78°W	*A. hyacinthus*	072099RM2	3.4366	0.0010	53	1.1405	0.0005	145.5	1.0	0.1215	0.1065	0.0001	12223	25	CAMS76147	10750	10400	30
CHR 7-3-2	1.99°N	157.78°W	*A. hyacinthus*	040402RM1	3.4910	0.0010	51	1.1414	0.0004	146.1	1.0	0.1170	0.1025	0.0002	11730	19	CAMS77435	10340	9990	30
CHR 7-4-3	1.99°N	157.78°W	*A. hyacinthus*	072099RM4	3.3209	0.0010	49	1.1384	0.0004	143.3	1.0	0.1232	0.1083	0.0001	12433	27	CAMS76149	10820	10470	30
CHR 7-4-5	1.99°N	157.78°W	*A. hyacinthus*	071003RM2	4.0428	0.0010	21	1.1422	0.0007	147.5	1.0	0.1269	0.1111	0.0002	12785	30	CAMS75380	11300	10950	30
CHR 7-5-2A	1.99°N	157.78°W	*A. hyacinthus*	072099RM6	4.1863	0.0010	27	1.1357	0.0003	140.7	1.0	0.1267	0.1116	0.0002	12838	47	CAMS76138	11300	10950	30
CHR 7-5-2A																	CAMS76151	11420	11070	30
CHR 7-5-2A																	CAMS77447	11350	11000	30
CHR 7-6-1	1.99°N	157.78°W	*A. hyacinthus*	071003RM3	3.9260	0.0010	34	1.1411	0.0007	146.4	1.0	0.1288	0.1129	0.0002	12995	28	CAMS76148	11500	11150	30
CHR 7-6-1																	CAMS76156	11430	11080	30
CHR 7-6-3.1	1.99°N	157.78°W	*A. hyacinthus*	072099RM5	3.7650	0.0010	32	1.1355	0.0003	140.6	1.0	0.1276	0.1124	0.0002	12942	48	CAMS76142	11420	11070	30
CHR 7-6-3.2																	CAMS81549	11450	11100	30
CHR 7-7-1.1	1.99°N	157.78°W	*A. hyacinthus*	030300RM3	3.6230	0.0010	34	1.1372	0.0006	142.6	1.0	0.1349	0.1187	0.0001	13709	24	CAMS77010	12080	11730	30
CHR 7-7-2A.1	1.99°N	157.78°W	*A. hyacinthus*	101599RM2	3.4371	0.0010	32	1.1427	0.0005	148.3	1.0	0.1327	0.1161	0.0001	13397	33	CAMS76140	11800	11450	30
CHR 7-7-3A.1	1.99°N	157.78°W	*A. hyacinthus*	040402RM2	3.6050	0.0010	17	1.1432	0.0005	148.7	1.0	0.1325	0.1159	0.0002	13365	21	CAMS77429	11770	11420	30
ARAKI	Reservoir age for Araki data is 365 yr																			
AK-BC-2	15.63°S	166.93°E	*Favia stelligera*	112503TC4	2.4369	0.0014	9	1.1410	0.0010	144.0	1.5	0.0765	0.0671	0.0001	7518	17	CAMS 112217	6895	6530	30
AK-BD-2	15.63°S	166.93°E	unidentified sp.	102803TC5	1.9947	0.0007	10	1.1263	0.0006	139.9	0.9	0.3186	0.2829	0.0003	36014	43	CAMS 99632	30690	30325	210
AK-BD-2																	CAMS 104452	30360	29995	240
AK-BD-3	15.63°S	166.93°E	*Porites*	102903TC1	3.9029	0.0013	8	1.1268	0.0005	139.8	0.8	0.3071	0.2725	0.0003	34467	39	CAMS 99022	29090	28725	190
AK-BD-3																	CAMS 104453	29700	29335	220
AK-BD-4	15.63°S	166.93°E	*Porites*	102903TC2	2.7232	0.0007	29	1.1274	0.0005	140.9	0.8	0.3152	0.2796	0.0003	35518	43	CAMS 99633	31110	30745	220
AK-BD-5	15.63°S	166.93°E	*Porites*	062603TC2	2.6362	0.0009	13	1.1264	0.0005	140.1	0.8	0.3204	0.2844	0.0005	36247	74	CAMS 99015	31670	31305	260
AK-BD-9	15.63°S	166.93°E	*Porites lutea*	102903TC6	2.8262	0.0008	734	1.1249	0.0005	139.8	0.8	0.3458	0.3074	0.0003	39759	42	CAMS 99024	35090	34725	400
AK-BD-10	15.63°S	166.93°E	*Favia stelligera*	010803RM1	2.5785	0.0005	12	1.1263	0.0004	141.3	0.6	0.3457	0.3069	0.0003	39684	50	CAMS 93343	35090	34725	430
AK-BD-10																	CAMS 99637	35410	35045	370
AK-BD-11	15.63°S	166.93°E	*Porites lutea*	063003TC3	2.6913	0.0006	299	1.1256	0.0004	140.0	0.8	0.3361	0.2986	0.0004	38401	58	CAMS 99016	32900	32535	300
AK-BD-11																	CAMS 104454	33390	33025	350
AK-L-1	15.63°S	166.93°E	*Favia stelligera*	010803RM2	2.1286	0.0004	16	1.1310	0.0004	144.1	1.1	0.3022	0.2672	0.0003	33677	39	CAMS 93342	29730	29365	230
AK-L-1																	CAMS 99636	29460	29095	180
AK-K-1	15.63°S	166.93°E	*Porites*	112403TC1	3.8042	0.0011	27	1.1273	0.0007	141.0	1.1	0.3206	0.2844	0.0003	36240	46	CAMS 104459	32140	31775	300
AK-K-1																	CAMS 106898	32130	31765	490
AK-K-2	15.63°S	166.93°E	*Platygyra lamellina*	042203TC2	2.4537	0.0005	24	1.1279	0.0005	141.7	1.5	0.3206	0.2842	0.0003	36216	49	KIA 24977	30980	30615	150
AK-F-1	15.63°S	166.93°E	*Favia*	082504TC1	2.8052	0.0008	13	1.1276	0.0007	141.3	1.0	0.3195	0.2834	0.0004	36091	67	CAMS 106896	32250	31885	500
AK-F-1																	CAMS 106893	32620	32255	530
AK-F-2	15.63°S	166.93°E	*Goniastrea*	082504TC3	2.5551	0.0006	9	1.1287	0.0006	142.5	0.9	0.3195	0.2831	0.0006	36047	96	CAMS 106897	31610	31245	460
AK-AA-1	15.63°S	166.93°E	*Favia stelligera*	082504TC4	2.2705	0.0005	15	1.1280	0.0004	142.5	0.7	0.3319	0.2942	0.0004	37724	68	CAMS 106890	34090	33725	630
AK-BE-1b	15.63°S	166.93°E	*Porites lutea*	063003TC4	2.7054	0.0006	337	1.1228	0.0005	139.7	0.7	0.3869	0.3446	0.0006	45689	93	CAMS 99018	42310	41945	960
AK-BE-1b				082604TC3	2.6771	0.0007	300	1.1252	0.0006	142.5	0.9	0.3877	0.3446	0.0006	45681	98				

Data table for radiocarbon calibration "Version Fairbanks0805"

Sample	Lat.	Long.	Species	U-series I.D.	U (ppm)	1σ	^{232}Th(ppt)	$[^{234}$U/^{238}U] act.	1σ	Initial δ^{234}U	1σ	$[^{230}$Th/^{238}U] act.	$[^{230}$Th/^{234}U] act.	1σ	Cal. age (yr BP)	1σ	^{14}C I.D.	Raw ^{14}C age (yr BP)	Res. corr. ^{14}C age (yr BP)	1σ
AK-AB-1	15.63°S	166.93°E	*Porites lutea*	042303TC1	2.5163	0.0005	57	1.1231	0.0005	141.1	0.7	0.4045	0.3602	0.0003	48273	49	KIA 24976	44410	44045	530
AK-AB-1				111803TC4	2.7484	0.0007	70	1.1226	0.0005	140.5	0.8	0.4036	0.3595	0.0003	48164	45				
ARA04-2D	15.63°S	166.93°E	*Goniastrea*	112304RM1	2.3337	0.0004	29	1.1299	0.0005	145.3	0.8	0.3477	0.3077	0.0009	39799	140	KIA 24978	35050	34685	230
ARA04-10D	15.63°S	166.93°E	*Favia*	112304TC2	2.4515	0.0004	9	1.1299	0.0005	145.4	0.7	0.3486	0.3085	0.0004	39930	58	KIA 24979	34570	34205	210
ARA04-11D	15.63°S	166.93°E	*Goniastrea*	102604LC5	2.4407	0.0011	36	1.1280	0.0005	143.7	0.8	0.3552	0.3149	0.0003	40923	54	KIA 24980	35640	35275	200
ARA04-17D	15.63°S	166.93°E	unidentified sp.	011805TC1	3.1012	0.0007	6	1.1289	0.0005	142.9	0.8	0.3232	0.2863	0.0003	36521	44	KIA 24981	31710	31345	150
ARA04-19D	15.63°S	166.93°E	*Porites*	011805TC2	3.3744	0.0009	94	1.1307	0.0005	144.7	0.8	0.3200	0.2830	0.0003	36031	44	KIA 24982	32070	31705	150
ARA04-22D	15.63°S	166.93°E	*Porites*	112304RM4	2.9510	0.0005	44	1.1323	0.0005	146.5	0.7	0.3203	0.2829	0.0004	36008	64	KIA 24984	31220	30855	140
ARA04-40E	15.63°S	166.93°E	*Platygyra*	102604RM4	2.4933	0.0005	10	1.1236	0.0005	142.1	0.7	0.4110	0.3658	0.0003	49203	45	KIA 24987	45160	44795	570
ARA04-43E	15.63°S	166.93°E	*Porites*	092204LC2	2.8368	0.0007	17	1.1252	0.0005	143.5	0.7	0.4048	0.3597	0.0006	48183	102	KIA 24988	46060	45695	630
ARA04-44E	15.63°S	166.93°E	*Porites*	092204LC3	3.1435	0.0011	69	1.1262	0.0006	144.7	0.9	0.4064	0.3609	0.0007	48378	112	KIA 24989	44750	44385	550
ARA04-71E	15.63°S	166.93°E	*Favia*	092304LC1	2.2226	0.0008	27	1.1258	0.0005	142.2	0.8	0.3729	0.3312	0.0005	43519	82	KIA 24991	38860	38495	380
ARA04-73E	15.63°S	166.93°E	unidentified sp.	092304LC2	2.1453	0.0005	14	1.1270	0.0005	143.9	0.8	0.3774	0.3348	0.0005	44098	83	KIA 24992	39710	39345	310
ARA04-75E	15.63°S	166.93°E	*Porites*	092304LC3	2.9473	0.0005	27	1.1254	0.0005	142.3	0.7	0.3820	0.3395	0.0006	44850	90	KIA 24993	41710	41345	390
ARA04-77E	15.63°S	166.93°E	unidentified sp.	092304LC4	2.6076	0.0005	8	1.1280	0.0005	144.9	0.8	0.3759	0.3333	0.0005	43840	86	KIA 24994	39700	39335	320
ARA04-85E	15.63°S	166.93°E	*Goniastrea*	092304LC5	2.5620	0.0005	4	1.1262	0.0004	142.8	0.7	0.3727	0.3310	0.0004	43474	72	KIA 24995	40460	40095	330
SANTO	*Santo Island samples used to supplement neighboring Araki Island reservoir age computation																			
S-C-4*	15.60°S	166.80°E	unidentified sp.	082304RM5	2.9044	0.0007	17	1.1490	0.0004	149.5	0.6	0.0136	0.0118	0.0001	1249	10	CAMS112210	1885	1520	30
S-T-2*	15.60°S	166.80°E	unidentified sp.	082704RM3	2.5864	0.0006	42	1.1479	0.0005	149.4	0.8	0.0352	0.0307	0.0002	3352	17	CAMS112212	3490	3125	35
S-W-2*	15.60°S	166.80°E	unidentified sp.	083004RM1	2.4537	0.0008	72	1.1473	0.0007	149.2	1.0	0.0471	0.0410	0.0003	4521	29	CAMS112213	4315	3950	30
S-X-1*	15.60°S	166.80°E	unidentified sp.	082704RM4	2.5621	0.0006	91	1.1472	0.0006	149.4	0.8	0.0537	0.0468	0.0002	5182	21	CAMS112214	4775	4410	35

Note:

Coral species -- "*A.*" represents *Acropora*; "*M.*" represents *Montastrea*; "*P.*" represents "*Porites*". "[ ] act." represents activity ratio.

Calendar ages were determined by ^{230}Th/^{234}U/^{238}U method by PLASMA 54 at LDEO (Mortlock et al. 2005) and were calculated using the following equation

$$\left[^{230}\text{Th}/^{234}\text{U}\right] = \frac{1 - e^{-\lambda_{230}*t_1}}{[^{234}\text{U}/^{238}\text{U}]} + \left(1 - \frac{1}{[^{234}\text{U}/^{238}\text{U}]}\right) * \frac{\lambda_{230}}{\lambda_{230} - \lambda_{234}} * \left(1 - e^{-(\lambda_{230} - \lambda_{234})*t_1}\right)$$

In all calculations, we use decay constants of λ_{230} = 9.1577 x 10^6 year^{-1} and λ_{234} = 2.8263 x 10^6 year^{-1} (Cheng et al., 2000).

^{14}C ages are based on the definition in Stuiver and Polach (1977).

"CAMS" represents ^{14}C dates performed at Lawrence Livermore National Laboratory, University of California.

"KIA" represents ^{14}C dates performed in the Leibniz Laboratory for Dating and Isotope Analyses, Christian-Albrechts-Universität, Kiel, Germany.

"WHOI" represents ^{14}C dates performed in the National Ocean Sciences Accelerator Mass Spectrometry Facility at Woods Hole Oceanographic Institution.